scientific reports

Check for updates

OPEN

Machine learning predictions for enhancing engine performance and emission using aluminum oxide nano additives in castor biodiesel

Murugu Nachippan[1], P. Pathmanabhan[1], Beemkumar Nagappan[2], Vijay J. Upadhye[3], Nandagopal Kaliappan[4,7]✉, V. Balaji[5] & K. Kamakshi Priya[6]

This study investigates the role of aluminum oxide nano-additives in enhancing the performance and reducing the environmental footprint of a B30 castor biodiesel blend in a compression ignition (CI) engine, emphasizing principles of green and sustainable chemistry. With global concerns over emissions and the depletion of fossil fuels, there is an urgent need for cleaner and more efficient alternative fuels. Biodiesel derived from non-edible sources, such as castor oil, presents a sustainable solution, but improvements in its combustion efficiency and emissions profile are crucial for widespread adoption. In this research, aluminum oxide nanoparticles were incorporated into a B30 biodiesel blend to enhance combustion properties, reduce ignition delay, and significantly mitigate harmful emissions, including carbon monoxide (CO), hydrocarbons (HC), and nitrogen oxides (NOx). The biodiesel was synthesized through the transesterification of castor oil, which is rich in ricinoleic acid, and tested on a Kirloskar diesel engine operating at a constant speed of 1500 rpm under varying load conditions. Results demonstrated that the nano-additive-infused biodiesel blend outperformed conventional diesel in terms of fuel economy, atomization, vaporization, and overall combustion efficiency. Additionally, the use of aluminum oxide nanoparticles reduced brake-specific fuel consumption (BSFC) and pollutant emissions. To further optimize engine performance and minimize emissions, a machine learning framework was applied, comparing algorithms such as Random Forest and XGBoost. The analysis identified XGBoost as the most accurate predictive tool, offering valuable insights for optimizing engine parameters. This work highlights the application of green and sustainable chemistry through the integration of nano-additives and advanced data analytics to develop cleaner, more efficient biodiesel fuels, contributing to the global shift toward environmentally friendly energy solutions.

Keywords Castor biodiesel, Aluminium oxide, Machine learning model, Random forest, XG Boost, Clean energy

Small and large-scale industrial operations, domestic energy, and transportation use compression ignition (CI) engines. Biodiesel and its blends with fossil diesel reduce their environmental impact. Adding biodiesel, a sustainable fuel, reduces CO_2, PM, and NOx emissions, addressing air quality concerns in energy production. Biodiesel may reduce greenhouse emissions and replace fossil fuels. Camelina, carinata, and pennycress are preferred biofuel sources as non-food crops. While biodiesel is greener than diesel in CI engines, it increases nitrogen oxides. Adding nanoparticles to biodiesel improves engine performance and reduces emissions by enhancing fuel thermophysical characteristics and heat transmission. This biodiesel reduces NOx by promoting complete combustion[1]. Blends of biodiesel and diesel with alumina nanoparticles improve CI engine

[1]Department of Automobile Engineering, Easwari Engineering College, Chennai, Tamilnadu, India. [2]Department of Mechanical Engineering, Faculty of Engineering and Technology, JAIN (Deemed-to-be University), Bengaluru, Karnataka 562112, India. [3]Parul Institute of Applied Scienes, Parul University, PO Limda, Tal. Waghodia, District Vadodara, Gujarat, India. [4]Department of Mechanical Engineering, Haramaya Institute of Technology, Haramaya University, Dire Dawa, Ethiopia. [5]Department of Mechanical Engineering, Vel Tech Rangarajan Dr. Sagunthala R&D Institute of Science and Technology, Chennai, India. [6]Department of Physics, Saveetha School of Engineering, SIMATS, Saveetha University, Chennai, Tamil Nadu, India. [7]Department of Food Technology, Dhanalakshmi Srinivasan Engineering College, Coimbatore, India. ✉email: raghugavaskarr@gmail.com

performance, boosting torque, power, efficiency, and reducing emissions. Alumina nanoparticles enhance fuel burning and energy conversion[2]. Blending coffee husk oil methyl ester with diesel reduced CO, HC, and smoke opacity levels, showing promise as renewable fuel[3]. Tallow oil biodiesel blends showed similar brake power but higher fuel consumption due to lower heating value[4]. Higher fuel injection pressure improved efficiency and reduced emissions in Nahar oil biodiesel, making it a sustainable alternative[5]. Using Taguchi's L9 array, adding hydrogen peroxide to Jatropha biodiesel improved performance and reduced emissions[6]. Biodiesel with cerium oxide, alumina, and titanium oxide nanoparticles improves combustion while reducing emissions and enhancing efficiency[7]. Adding ethanol and alumina nanoparticles to biodiesel decreases CO and HC emissions, indicating higher combustion efficiency. However, this mixture increases CO_2 and NOx emissions. The CO_2 increase indicates complete combustion, while NOx increases due to higher combustion temperatures[8]. Despite these developments, the transport sector relies heavily on petroleum-powered internal combustion engines. Even as battery electric vehicles emerge, ICEs will dominate transport energy through 2040, making engine efficiency and emission control crucial[9]. Biodiesel from waste benefits both environment and fuel industry sustainability. Fish waste oil biodiesel showed similar performance to other biodiesels with decreased emissions, necessitating life-cycle analysis for environmental impacts[10].

Relative studies on nano additive in biodiesel

Multi-walled carbon nanotube blending with palm-oil biodiesel enhanced combustion characteristics and flammability limits but raised nitrogen oxide emissions[11]. Biodiesel blending with cerium oxide nanoparticles increased engine performance and lowered emissions[12]. Titanium oxide nanoparticles in palm and sesame oil biodiesel improved lubricity, reduced wear and friction, enhancing performance and reducing emissions[13]. Cerium oxide nanoparticles improve efficiency and fuel economy[14]. Adding titanium oxide nanoparticles to waste cooking oil biodiesel improves performance and reduces emissions, showing potential as a renewable energy option[15]. Zinc oxide nanoparticles improve soybean biodiesel properties but increase NOx emissions[16]. Graphene-based nanoparticles reduce smoke and NOx through oxygen-functionalized groups[17]. Citrus oil biodiesel with carbon nanotubes and cerium oxide reduces CO and HC emissions[18]. Manganese and cobalt oxide nanoparticles enhance brake thermal efficiency and reduce emissions[19]. Lemon and orange peel biofuels with carbon nanotubes and cerium oxide lower emissions, demonstrating benefits of biodiesel-nanoparticle blends[20]. Together, these results show that nanoparticle-enhanced biodiesel improves engine performance while reducing emissions. Methyl esters from Tevetia peruviana, Honne, and Neem oils tested in normal engines showed low exhaust gas temperature[21]. Engine brake thermal efficiency and emissions for 5% graphene nanoparticles in linseed biodiesel exceeded diesel performance[22]. Zinc oxide nanoparticles in Mahua biodiesel produced good performance and decreased emissions[23]. Alumina nanoparticles enhanced diesel–biodiesel blend combustion. The grasshopper optimization algorithm determined optimal ethanol-biodiesel-diesel mixtures for efficiency and lower emissions[24,25]. Graphene and graphite nanoparticles in waste cooking oil biodiesel improved BTE and reduced nitrogen oxide emissions[26]. Bael biodiesel with dimethyl carbonate reduced CO and HC emissions[27]. Carbon nanotubes in peanut oil biodiesel improved performance and reduced emissions[28]. Graphene quantum dots in waste fish oil biodiesel enhanced engine performance[29]. Machine learning and AI techniques improved fuel composition, engine performance, and emissions reduction[29]. Hybrid nanoparticles of magnesium oxide and alumina with water-in-diesel emulsions showed optimal proportions through deep neural network optimization[30]. Metal-oxide nanoparticles proved successful in compression ignition engines. Deep Learning, Neural Networks, k-nearest Neighbors, and Support Vector Machines predicted engine reactions, reducing pollution and improving performance[31]. Engine settings improved using food waste oils and hybrid Adaptive Neuro-Fuzzy Inference System achieved higher efficiency[32]. Nanoparticles in waste oil biodiesel demonstrated better combustion efficiency and lower emissions[29]. These findings demonstrate how algorithms and nanoparticles improve engine efficiency in biodiesel applications. Machine Learning and Explainable AI guided experimental investigations for optimal fuel composition[33]. This study aims to optimize compression ignition engine performance using aluminium oxide nano-additives in B30 castor biodiesel blend, focusing on improving combustion efficiency, engine power, and reducing emissions while minimizing fuel consumption. Studies show Al_2O_3 nano-additives act as oxygen buffers, reducing CO and HC emissions, while enhancing fuel–air mixing for better combustion. Limited research has explored ML integration for predicting nano-additive blended biodiesel impacts, with studies focusing mainly on conventional biodiesel models. While machine learning models have been used for nano-biodiesel predictions, comparative analyses of Random Forest and XGBoost remain limited. Optimizing ML parameters for nano-biodiesel predictions and validating with engine experiments need further investigation. The study addresses a research gap by combining nano-additive enhancements with machine learning for performance optimization. Table 1 shows the analysis of nano additive blended biodiesel performance and emission study in CI engine.

Materials and methods

Preparation of nano suspended castor biodiesel

Castor oil is rich in ricinoleic acid, and so it is a resourceful raw material for making biodiesel. Its uniqueness in esterifying only with methanol further assures that production cost is extremely low. Everything, from the feedstock to biodiesel and glycerol, very much depends on the transesterification process, which by itself is majorly dependent on free fatty acid concentration, type of alcohol, molar ratio, type of catalyst, catalyst loading, and the reaction temperature[34]. From this experiment, a determined free fatty acid content of only 0.72% was established, while the saponification value was given at 74.15 mg KOH/g. The relatively low free fatty acid content in castor oil allows it to be used either in one-step transesterification or a base-catalyzed transesterification method. The optimum conditions of this reaction are achieved by maintaining the alcohol at 9:1 molar ratio with the oil and catalyst concentration at 1% KOH[35]. These conditions allow an efficient process of transesterification

Base fuel	Test fuel	Inference	Results						
			Performance		Emission				
			BTE	BSFC	HC	CO	NOx	Smoke	References
Diesel (D100)	TiO_2 + Mahua biodiesel (B20)	TiO_2 improves combustion efficiency CO and HC emissions reduced Slight NOx reduction vs diesel	↓ 4%	NA	↓46.6%	↓ 46.6%	↓ 2.3%	NA	[8]
Soybean biodiesel (SBME100)	ZnO + Soybean biodiesel (SBME25)	Emissions (HC, CO, smoke, CO_2) reduced NOx increased due to higher combustion temperature Best performance with SBME25ZnO50 at CR 21.5	↑ 23.2%	↓ 26.6%	↓ 32.2%	↓ 28.1%	↑ 43.2%	↓ 22.5%	[16]
Palm Biodiesel + Sesame Biodiesel (B100)	TiO_2 + Palm Sesame (B30)	B30 + DMC improved BTE and lowered carbon emissions B30 + TiO_2 enhanced engine performance significantly	↑ 4.97%	↓ 8.48%	↑ 40%	↑ 50%	↓ 42%	↓ 44%	[13]
Lemon Peel oil Biodiesel (LPO20)	CeO_2 + Lemon Peel oil Biodiesel (LPO20)	CNTs and CeO_2 added to lemon/orange oil blends BTE slightly lower than diesel BSEC reduced NOx reduction was marginal with all blends	↑ 24%	↓ 26%	↓ 68%	↓ 33%	↓ 30%	↓ 44%	[20]

Table 1. Analysis of nano additive blended biodiesel performance and emission study in CI engine.

Specification of "Kirloskar Variable Compression Ratio Engine"			
Bore	87.5 mm	Stroke	110 mm
Maximum engine power output: 3.5 kW			
Compression ratio range: 12:1–18:1			
No of cylinders: Single-cylinder			
Type of stroke: Four stroke			
Injection system: Direct injection, Solenoid driven injector			
Cooling system: Water cooled			
Dynamometer: Eddy current, water-cooled with a loading unit			

Table 2. Test engine specification.

so that biodiesel production is promoted with relatively minimal complications from free fatty acids. The overall time for the entire transesterification process is 45 min, and stirring at a speed of 150 rpm is observed. Alumina nano additive suspension in castor biodiesel of various proportions—10, 40, 70, and 100 ppm—was subjected to ultra sonification to improve the suspension of nano additives in castor biodiesel[36]. The nano additives were dispersed in the castor biodiesel blend using an ultrasonication process to ensure homogeneous mixing and stability. The ultrasonication was carried out using a probe-type ultrasonicator operating at 20 kHz frequency and 500 W power. The sonication duration was optimized by varying the time between 15 and 60 min, and the best dispersion stability was achieved at 45 min. The temperature during ultrasonication was maintained below 50 °C to prevent agglomeration of nanoparticles. After 45 min, it was observed that dispersion stability was poor and it leads to re-agglomeration. An experimental work involving a Kirloskar diesel engine was carried out, which utilizes a single-cylinder, four-stroke, direct injection, air-cooled compression ignition engine. The experiments were well controlled and carried out with different fuel blends at a constant speed of 1500 rpm to assess the performance and emissions under standardized conditions.

Experimental setup

The Common Rail Direct Injection engine with Variable Compression Ratio is one of the state-of-the-art and highly sophisticated products designed in accordance with the best standards of testing the engines. It is a 4-stroke and single-cylinder, water-cooled Kirloskar engine, making sure the cooling is sufficient and efficient. The stroke of the engine is 110 mm, and the bore is 87.5 mm, with a total displacement of 661 cc. This engine is rated at 3.5 kW with a speed of 1500 rpm, thus has the capability to provide high-quality performance in different forms of applications[37]. The study evaluated compression ratios of 12:1, 14:1, 16:1, and 18:1. A compression ratio of 16:1 was chosen to optimize combustion, improving fuel economy and emissions. At this ratio, both WCB20 and petroleum diesel showed reduced brake-specific fuel consumption[38]. While a higher ratio of 18:1 improved brake thermal efficiency and combustion, it also led to increased CO_2 and NOx emissions[39]. The compression ratio range of the engine is 16:1, which helps in further controlling the combustion process and achieving maximum fuel economy. This engine uses an eddy-current type of water-cooled dynamometer to ensure precision and repeatability in testing. The product uses "Engine Soft" software, a very high-level performance analysis software of an engine that gives the best overview of engine performance. The Table 2 mentions the specification of test engine and Fig. 1 shows the schematic layout of test engine configuration.

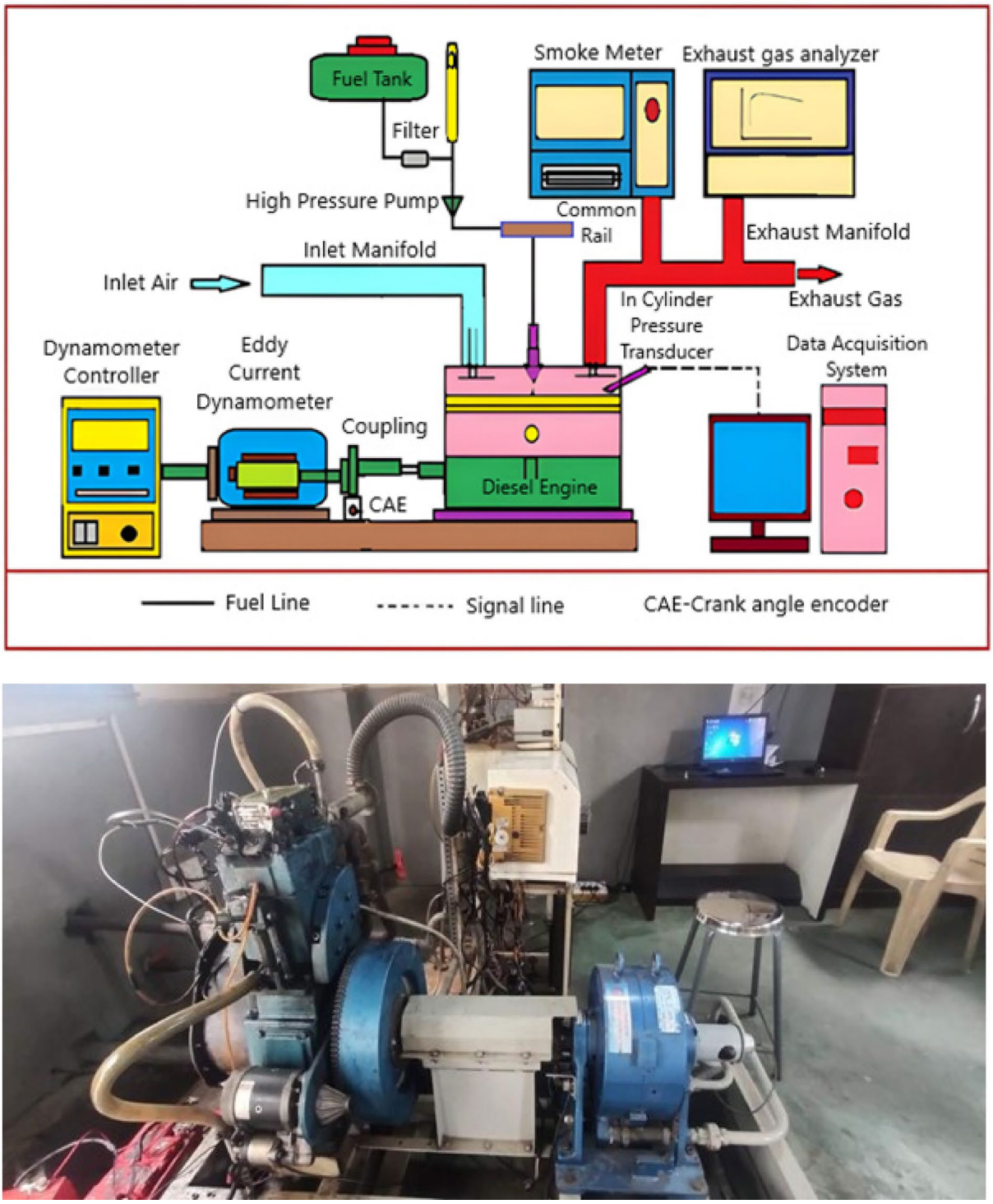

Fig. 1. Schematic layout and pictorial view of test engine configuration.

Uncertainty analysis

The Root Sum Square (RSS) method is used to determine the overall uncertainty of the measurement system by combining the individual uncertainties of each parameter. The assumption here is that each measurement contributes equally to the total uncertainty.

Table 3 enumerates and summarizes all the estimated uncertainties for each measurement test in this performance-emission study of the compression ignition engine run with biodiesel from castor oil and alumina nano additives. For any given measured parameter, the uncertainties may be sourced from a variety of factors, which is quantified in order to ascertain its reliability.

Parameter	Uncertainty sources	Uncertainty
Brake thermal efficiency (BTE)	Pressure sensor	± 0.7%
	Flow meter	± 0.3%
Brake specific fuel consumption (BSFC)	Flow meter	± 0.3%
Carbon monoxide (CO)	Gas analyzer	± 0.015%
Hydrocarbons (HC)	Gas analyzer	± 1 ppm
Nitrogen oxides (NOx)	Gas analyzer	± 2 ppm
Smoke	Smoke meter	± 1%

Table 3. Uncertainty sources in experimentation.

In the research, an important measure-the combined uncertainties on key measurements-is provided through calculated overall uncertainty of 2.58%. The measurements incorporated precision for determining parameters, such as brake thermal efficiency, brake-specific fuel consumption, and emissions (for example, carbon monoxide, hydrocarbons, NOx, and smoke levels). The quantified uncertainty leads to a degree of confidence in the accuracy and reliability of the experimental findings, thus ensuring that the results are robust and valid for evaluating engine performance and emissions.

$$Totaluncertainty(\text{ BTE }) = \sqrt{(0.7\%)^2 + (0.3\%)^2}$$

$$U(\text{BTE}) = \sqrt{0.49\% + 0.09\%} = \sqrt{0.58\%} \approx 0.76\%$$

$$Overall\ Uncertainty \approx \sqrt{(0.76\%)^2 + (0.3\%)^2 + (0.015\%)^2 + (1\%)^2 + (1\%)^2 + (2\%)^2}$$

$$U(Overall) = \sqrt{0.5776\% + 0.09\% + 0.000225\% + 1\% + 1\% + 4\%} = \sqrt{6.667825\%} \approx 2.58\%$$

Machine learning models

The application of XGBoost and Random Forest models for predicting internal combustion (IC) engine performance and emissions is explored across several studies, highlighting their effectiveness and versatility. Random Forest has been successfully applied to predict particulate emissions from gasoline direct injection (GDI) engines, demonstrating its capability to model complex emission parameters such as particle size and concentration, with insights into the effects of fuel chemistry on emissions formation[40]. The integration of Random Forest with XGBoost and Artificial Neural Networks (ANN) in ensemble models has been shown to enhance prediction accuracy, outperforming single machine learning models in terms of error reduction and generalization[41]. In urban vehicular emissions prediction, Random Forest models have shown high reliability, explaining up to 97% of data variance for fuel consumption and emissions like CO_2, CO, and NOx, although less effective for hydrocarbons due to vehicle model diversity[42]. Specifically, XGBoost has been noted for its high prediction accuracy in engine performance and emissions, achieving an R2-Score of 0.999, which underscores its precision in modeling complex engine dynamics and emissions characteristics[43]. These studies collectively illustrate the potential of ensemble machine learning techniques, including XGBoost and Random Forest, in advancing the predictive capabilities for IC engine performance and emissions, offering significant improvements over traditional empirical models. To predict the performance and emission characteristics of the engine fuelled with castor biodiesel and Al_2O_2 nano-additives based on previous studies, Random Forest (RF) and Extreme Gradient Boosting (XGBoost) models were implemented. These models were selected due to their high accuracy, robustness in handling nonlinear relationships, and ability to capture complex interactions between input parameters. The dataset was compiled from experimental results obtained at varying engine loads, biodiesel blend ratios, and nano-additive concentrations.

Random forest model

Random Forest reduces the risk of overfitting and enhances stability by averaging the predictions from a variety of decision trees. By utilizing bagging and metrics like Gini impurity, feature importance analysis highlights the main factors influencing predictions. This synergy improves generalizability, making Random Forest a reliable tool for both prediction and feature analysis[44].

Random Forest combines N decision trees, each making predictions. y_i based on a subset of features X_i and a subset of data points. The final prediction is an average or vote across all trees:

$$\widehat{y} = \frac{1}{N}\sum_{i=1}^{N} y_i \tag{1}$$

Bagging is carried out using bootstrap sampling, and feature importance is typically evaluated with metrics like the decrease in Gini impurity or information gain. In tree-based splitting, each decision tree aims to reduce impurity measures such as Gini impurity or entropy when selecting features. The complete model is a weighted aggregate of the predictions made by the individual trees.

$$\widehat{y}RF = \sum_{i=1}^{N} w_i f_i(X) \tag{2}$$

where w_i represents the weight of the i_{th} tree and $f_i(X)$ is the prediction of the i_{th} tree.

XGBoost model

XGBoost is an optimized gradient boosting algorithm that improves efficiency and performance by incorporating second-order optimization and regularization. It minimizes the following objective function:

$$L = \sum l(y_i, \widehat{y_i}) + \sum \Omega(f_k)$$

where the first term represents the loss between actual and predicted values, and the second term is a regularization function that penalizes model complexity to prevent overfitting. To improve training efficiency, XGBoost approximates the loss function using a second-order Taylor expansion:

$$L \approx \sum \left(g_i f\left(x_i\right) + \frac{1}{2} h_i f^2\left(x_i\right)\right) + \Omega(\mathrm{f})$$

where g_i is the first derivative (gradient) of the loss function, and hih_ihi is the second derivative (Hessian). The model grows decision trees by selecting the best split based on a gain function, which measures the improvement from splitting a node:

$$Gain = \frac{1}{2}\left[\frac{\left(\sum_{i\in I_L} g_i\right)^2}{\sum_{i\in I_L} h_i + \lambda} + \frac{\left(\sum_{i\in I_R} g_i\right)^2}{\sum_{i\in I_R} h_i + \lambda} - \frac{\left(\sum_{i\in I} g_i\right)^2}{\sum_{i\in I} h_i + \lambda}\right] - \gamma$$

where I_L and I_R are the left and right child nodes, and λ and γ control regularization. The optimal weight for each leaf node is given by:

$$w_j^* = -\frac{\sum_{i\in I_j} g_i}{\sum_{i\in I_j} h_i + \lambda}$$

Ensuring efficient updates for tree nodes. XGBoost enhances model performance through L1 and L2 regularization, pruning unnecessary splits, and using parallel computation for faster execution. By combining these techniques, it achieves superior accuracy and scalability in classification and regression tasks[45].

Results and discussion

Brake thermal efficiency

Brake thermal efficiency depends significantly on load conditions and fuel composition. Besides, at lower loads, efficiency as well as combustion of the fuel is less than optimal. When load increasing from 0 to 75%, more will be the energy utilization from the fuel, with higher brake thermal efficiency. At 100% load, the brake thermal efficiency is slightly reduced due to higher heat dissipation leads to heat loss[46]. B30 biodiesel blend shows higher efficiency compared to other biodiesel blend and shows lower reductions in emissions compared to the diesel. Hence this blend is chosen as an optimal biodiesel blends for further experimentation with nano additive blended biodiesel. Similar trend is observed in a following study was observed that lemongrass oil biodiesel (B30) with 4% dibutyl ether showed optimal performance at CR 17.5, with reduced emissions except HC at higher loads[47]. Palm methyl ester (B30) in road vehicles reduced CO, HC, and PM, but slightly increased NOx, with fuel economy similar to B20[48]. Higher biodiesel content in B30 castor biodiesel than that of B10 makes certain benefits including low emission, better performance of the engine, higher fuel economy, and good performance in cold climate conditions[49]. The blends of B30 Castor biodiesel also have logistical advantages wherein it has a higher availability and better compatibility with the current diesel engine technologies which makes its adoption at a larger scale more feasible[50]. Nano-additives improve fuel atomization and vaporization, resulting in more complete combustion in the cylinder of an engine. Apart from raising the overall thermal efficiency, nano-additives minimize friction of moving parts of engines thus extending its life cycle and enhancing lubrication. For instance, combustion properties in B30 castor biodiesel blends are significantly enhanced by aluminum oxide nanoparticles. They serve as a catalyst that allows for the atomization and vaporization of fuel at an enhanced efficiency and completeness with respect to the combustion process. This secondary impact of the blends containing aluminum additives in the B30 castor biodiesel blend is an anti-oxidation/degradation role, thereby adding support to engine performance and longevity as well. Pure biodiesel has lower brake thermal efficiency than diesel primarily due to a lower calorific value and viscosity greater than that of diesel. However, the aluminum additives promote biodiesel blends, which significantly enhance combustion at higher concentrations of concentration due to better fuel oxidation. Better combustion efficiency in compensating for some of the inherent limitations in biodiesel happens to optimize engine performance. The catalytic impact of the additives enhanced the ignitability and flammability for concentrations of 40–100 ppm, hence leaving a synergistic efficiency advantage of 5.51% over the neat diesel. Additionally, at a concentration of 100 ppm, a high enhancement of 18.71% in the brake thermal efficiency over neat biodiesel was achieved primarily due to decreased soot formation and better flame propagation, which leads to more comprehensive combustion[51].

These research findings are to optimize the fuel composition and the use of catalytic additives, such as aluminum oxide nanoparticles, to maximize engine efficiency, reduce emissions, and increase the lifespan of the engine[52]. The fuel technologies that exhibit such developed properties can enhance the efficiency of a fuel as well as contribute towards environmental sustainability if incorporated into modern diesel engines.

Figure 2 shows the variation of Brake thermal efficiency of castor biodiesel blends and Alumina nano additive blended castor biodiesel.

Brake-specific fuel consumption

Brake Specific Fuel Consumption is an important indicator of the efficiency of the engine when producing work, and especially when different fuels or different blends are involved. At 25% and 50% loads, it means less efficient combustion and higher fuel consumptions per unit of work output. Here, the engine operates in a region where it definitely doesn't maintain its optimum efficiency condition, which increases its fuel consumption.

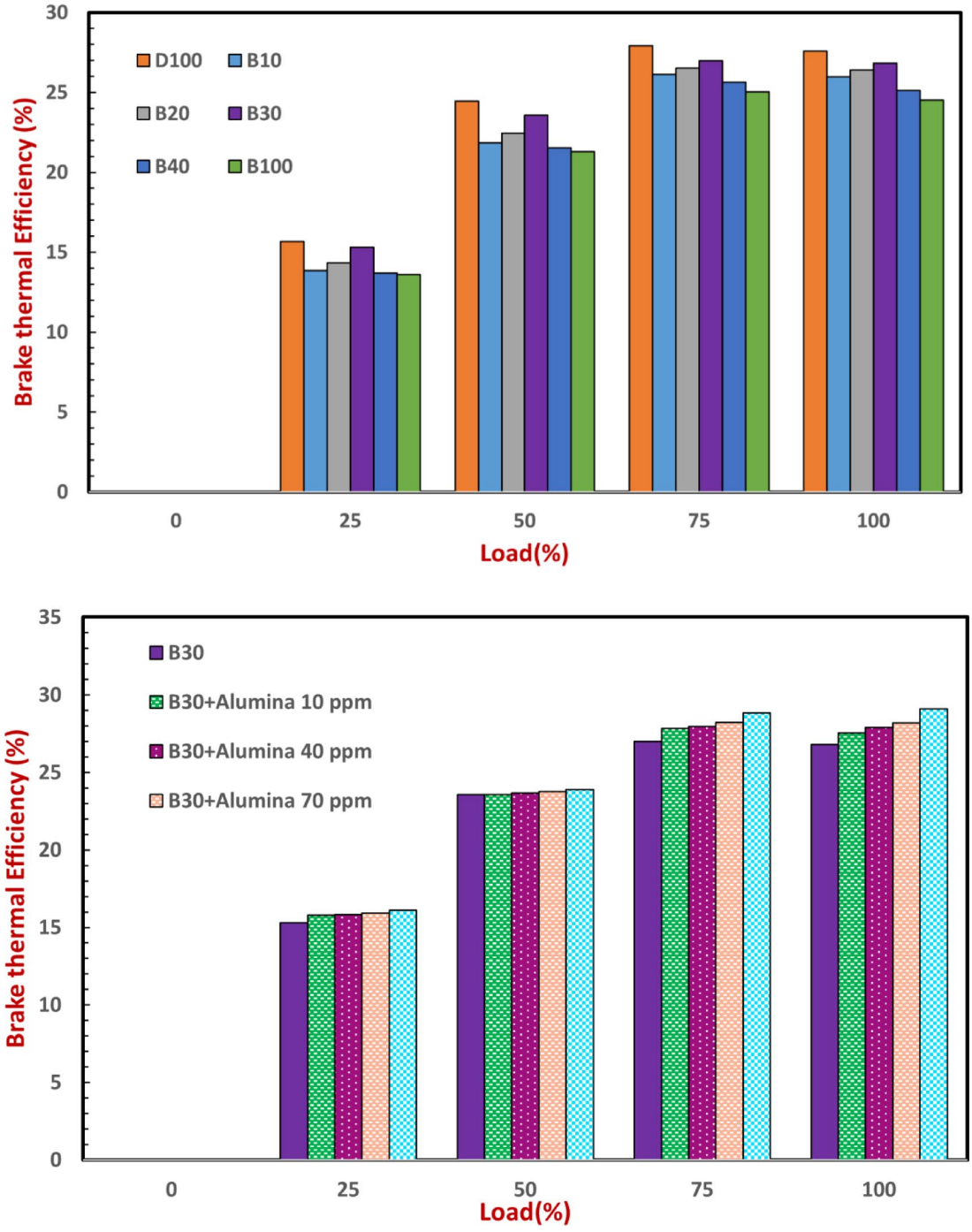

Fig. 2. Brake thermal efficiency of castor biodiesel blends and alumina nano additive blended castor biodiesel.

However, for 75% loads, the engine achieves maximum efficiency with a corresponding reduction in BSFC by consuming less fuel per unit of work[53]. BSFC varies with blend composition and combustion properties for neat diesel concerning the biodiesel blends. For B10 and B30 blends, BSFC is higher than that for neat diesel because of some specific characteristics of biodiesel, such as higher viscosity and lower calorific value that affect fuel atomization and energy release. Pure biodiesel, B100, has a rise in brake specific fuel consumption over regular diesel of 17.74%. This means that the energy density is lower and combustion less efficient for this biodiesel, which leads to higher consumption with respect to the same power output. Therefore, this is an indication of some need for optimization measures to make utilization of biodiesel more efficient. Therefore, the pure biodiesel is less fuel-efficient with respect to fuel intake, thereby eroding its relative cost competitiveness. The B30 castor biodiesel blend balances well in a way that it promotes emissions reduction while maintaining competitiveness in both fuel efficiency and vehicle performance. It further offers a larger quantity of emissions reduction with competitive engine efficiency and fuel economy in comparison to the B10 Biodiesel. The B30 blend achieves this through the optimized ratio of biodiesel to diesel content, thus increasing better combustion and utilization of fuel as compared to neat diesel[54]. Addition of aluminium oxide nanoparticles into biodiesel blends has proved to significantly enhance the combustion efficiency and lower brake specific fuel consumption. Al nanoparticles intensify fuel atomisation and vaporisation and produce better combustion, with less energy loss due to unburned fuel. Adding aluminium oxide nanoparticles to a B30 biodiesel blend was found to significantly reduce brake specific fuel consumption, indicating the presence of nanoparticles' function in improving fuel combustion and overall fuel efficiency.

Concentration of 10 ppm of aluminum oxide leads to 3.92% reduction in brake-specific fuel consumption as compared to neat diesel and increased concentration of 100 ppm has shown an incredible value of 24.51%[55]. The B30 biodiesel blend with a 100 ppm aluminium oxide ingredient demonstrated a notable reduction of 37.90% in brake specific fuel consumption compared to pure diesel. This substantial figure indicates efficiency enhancements due to the integration of aluminium oxide, which improves fuel atomisation and combustion completeness, hence facilitating fuel economy advancements and reducing energy loss in compression ignition engines. This is especially because of the new ignition and combustion processes initiated with the presence of aluminum, which reduced sooting formation and ensured better flame propagation. Figure 3 shows the variation of Brake Specific fuel consumption of castor biodiesel blends and Alumina nano additive blended castor biodiesel.

Carbon monoxide

Carbon monoxide is emitted in diesel engines resulting from the incomplete combustion, especially from conventional diesel that lacks sufficient oxygen to completely oxidize hydrocarbons. Diesel fuels have characterised high emissions of CO in general, mainly when there is a rich air–fuel mixture, as well as poor atomization under 100% engine loads[56]. The result of this incomplete combustion is that some carbon atoms in the fuel do not get fully oxidized and hence remain as CO, rather than getting oxidized to carbon dioxide (CO_2). By contrast, biodiesel and its blends like B10, B20, B30, and B100 are generally associated with lower CO emissions due to the reason that biodiesel contains oxygen within its chemical structure, and hence, its combustion gets enhanced to be more complete[57]. Consequently, there is a progressive reduction of CO in the mixtures with an increase in biodiesel concentration. For instance, B100 offers almost 28.33% less CO in combustion process compared to D100, which is due to higher oxygen content in the biodiesel, thus creating easier combustion of fuel. Still, B100 has its own list of disadvantages with it, such as higher viscosity and lower calorific value, hence, when cold starts occur, its combustion might be only partially complete under such specific conditions. The B30, which is a 30% biodiesel and 70% diesel mixture, comprises an ideal balance in reductions of emissions without sacrificing any combustion stability, making due benefit from the oxygen content in biodiesel as well as the reliable ignition properties of petroleum diesel[58]. Combustion efficiency is also highly improved by adding aluminum oxide nanoparticles to B30 blends. As a catalyst, alumina enhances fuel atomization, which further leads to complete combustion.

Alumina accelerates the oxidation, and therefore, CO emission is significantly mitigated. For example, when B30 is blended with 10 ppm of alumina, CO emission is found to be 37.54% lesser than pure diesel. However, B30 with 100 ppm of alumina reduces CO emission by 42.66%. If compared with alumina to B100, the results striking is that B30 with 100 ppm alumina reduces CO emissions by 23.33% compared with B100. This shows that biodiesel mixed with alumina nano-additives will not only burn efficiently but also reduce CO emissions considerably above that of pure biodiesel[59]. With alumina additives, B30 seems to be the best for the reduction of CO from diesel engines and can well be a cleaner, environmentally friendly alternative to the fuel, especially for high-load conditions where CO emissions are the highest. Figure 4 shows the variations in CO emissions of castor biodiesel blends and Alumina nano additive blended castor biodiesel.

Hydrocarbon emission

Hydrocarbon emissions, which primarily consist of unburned fuel and oil vapours, tend to increase with rising engine loads due to incomplete combustion and the use of richer air–fuel mixtures at higher loads. Diesel engines typically emit higher levels of hydrocarbons compared to biodiesel and biodiesel blends, which benefit from superior combustion characteristics and different fuel properties. Biodiesel's oxygen content plays a crucial role in promoting more complete combustion, reducing the emission of unburned hydrocarbons compared to diesel[60]. However, even biodiesel and its blends experience an increase in HC emissions at 100% engine loads, as the combustion process becomes less efficient. Biodiesel blends like B30 (30% biodiesel, 70% diesel) have emerged as a practical and effective solution for reducing HC emissions while maintaining engine performance and compatibility with existing diesel infrastructure. B30 offers a balanced composition that enhances combustion efficiency without requiring significant engine modifications. This blend also performs well in cold conditions,

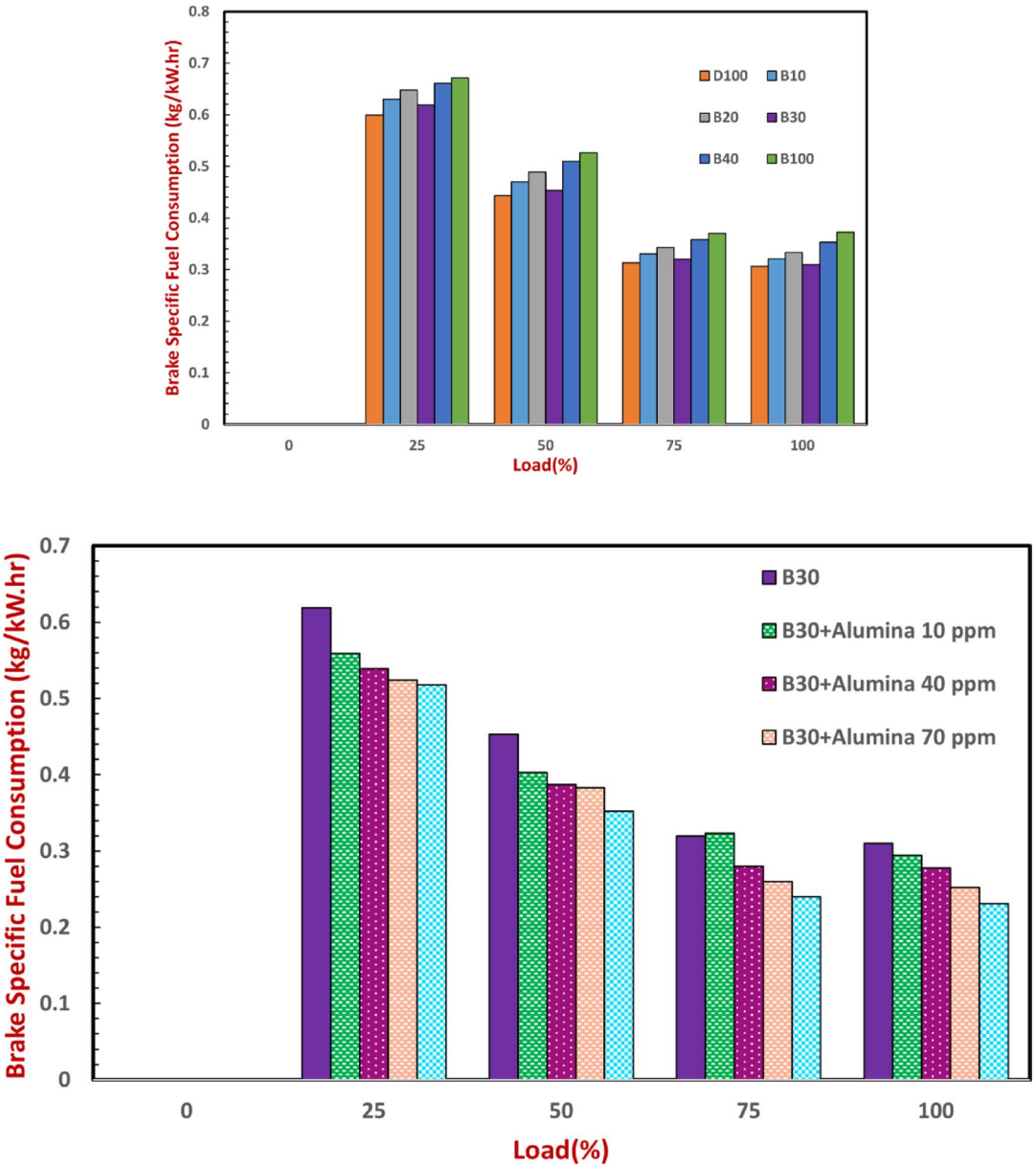

Fig. 3. Brake specific fuel consumption of castor biodiesel blends and Alumina nano additive blended castor biodiesel.

addressing fuel gelling and cold-start issues typically seen in higher biodiesel concentrations[61]. In addition to the inherent benefits of biodiesel, the inclusion of aluminum oxide nano-additives in B30 biodiesel blends can further reduce HC emissions by improving the combustion process. Alumina nano-particles enhance the burning efficiency significantly by improving atomization of fuel and easy exhaust of the fuel air, mixture thereby reducing, more significantly, the un-burnt hydrocarbons formed in the exhaust system. Moreover, aluminium nano-additives improved the thermal conductivity together with the heat transfer feature in the fuel, meaning to promote more effective dispersion during combustion. This limits any heat losses and thus additional HC emissions due to completeness of fuel combustion[62]. The impact of aluminum nano-additives on hydrocarbon emissions has been demonstrated through empirical results. It was found that neat biodiesel resulted in 23.75% less hydrocarbon (HC) emissions than pure diesel due to its oxygen-rich composition. The high oxygen level in the composition allows for a better combustion and the use of cleaner fuel, thus reducing the occurrence of hydrocarbon in the exhaust emission. This feature of biodiesel makes it a clean fuel choice for the reduction in HC emissions in compression ignition engines. However, when aluminum additives are introduced into a B30 biodiesel blend, the reduction in HC emissions becomes even more pronounced.

A B30 biodiesel blend with 10 ppm of aluminum resulted in a 26.25% reduction in hydrocarbon (HC) emissions when compared to the pure diesel, and this is increased to 38.75% at 100 ppm concentration, and these enormous cuts can be attributed to its nature that has inherent catalytic characteristics along with improved

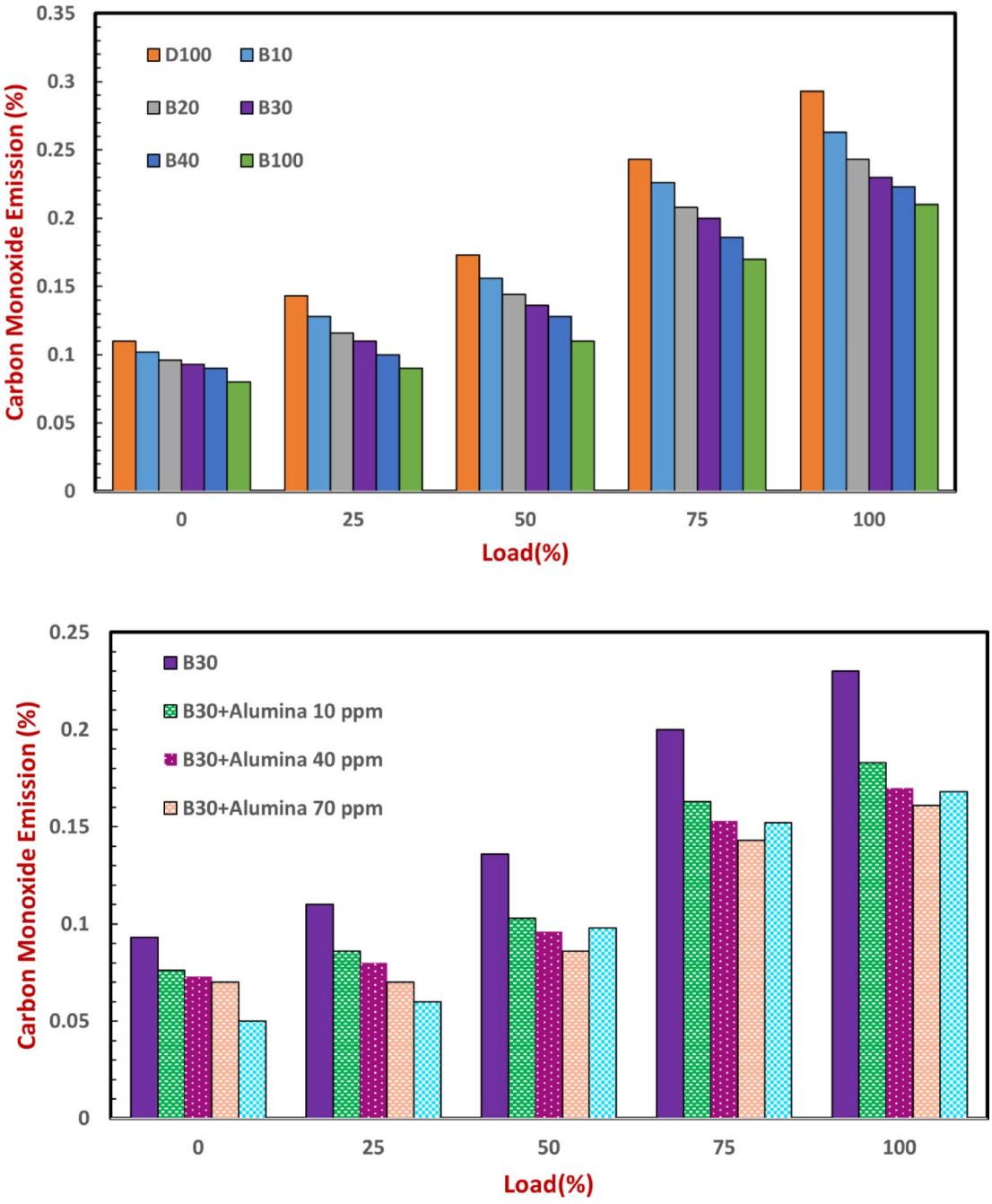

Fig. 4. CO emissions of castor biodiesel blends and alumina nano additive blended castor biodiesel.

atomization fuelling and air–fuel mixture integration. This advanced combustion process ensures that the burn will be complete and, hence, reduces residual hydrocarbons in the exhaust and improves the environmental productivity of the biodiesel blend. When comparing B30 with aluminum additives to pure biodiesel, the improvement is also significant. At a 10 ppm aluminum concentration, HC emissions are 3.28% lower than B100, and at 100 ppm, the reduction reaches 19.67%. Figure 5 shows the variations in HC emissions of castor biodiesel blends and Alumina nano additive blended castor biodiesel.

Nitrogen oxide emission

NOx emissions, which consist of nitrogen oxides (NO) and nitrogen dioxide (NO_2), generally tend to increase from 0 to 100% load as raising temperatures and pressure inside the combustion chamber enables a greater interaction between oxygen and nitrogen to result in higher NOx[63]. Generally, biodiesel and its blends typically produce more nitrogen oxide emissions than regular diesel, mainly due to the higher oxygen content as well as combustion properties of biodiesel, causing increased peak combustion temperatures, thereby facilitating the production of NOx. This is mainly due to biodiesel's higher oxygen content, which promotes complete combustion

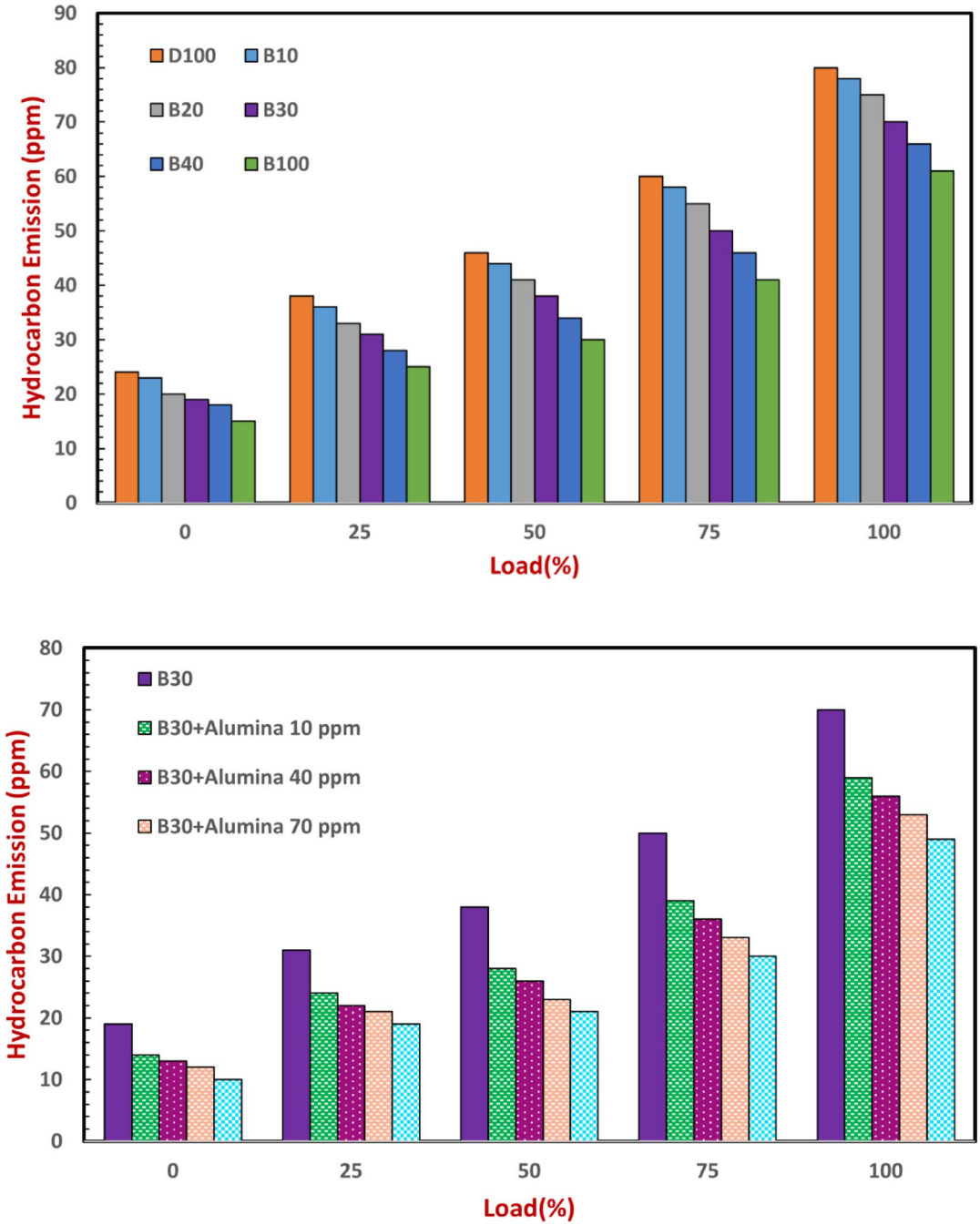

Fig. 5. HC emissions of castor biodiesel blends and alumina nano additive blended castor biodiesel.

but also increases combustion temperatures, fostering nitrogen oxide emissions formation. Additionally, biodiesel's lower cetane number, leading to longer ignition delays, further contributes to this NOx increase. B100 biodiesel causes an augmentation of 14.45% in NOx as compared with regular diesel; this is an important environmental concern despite the numerous advantages of biodiesel on the reduction of particulate matter, and carbon monoxide (CO) emissions. The increase in NOx is principally because of the larger oxygen contents of biodiesel that allow combustion at higher temperatures and favor the formation of NOx thus offering a trade-off between improved combustion efficiency and increased NOx emissions[64]. Alumina nano additives have shown potential in reducing NOx emissions in biodiesel blends by enhancing fuel atomization and lowering peak combustion temperatures. Empirical data reveal significant NOx reductions with increasing concentrations of alumina. For instance, a B30 blend with 70 ppm alumina reduces NOx by 17.63%, and a 100 ppm concentration results in a 22.10% reduction compared to neat diesel. These additives are particularly effective under high-load engine conditions, where NOx emissions are most challenging[65]. A B30 blend with 70 ppm alumina reduces NOx by 28.03%, while 100 ppm achieves a 31.82% reduction compared to neat biodiesel. This approach helps balance the environmental benefits of biodiesel with lower CO and particulate matter emissions, challenges of

higher NOx emissions, making biodiesel blends more viable for environmentally friendly, high-load engine operations[66]. Figure 6 shows variations in NOx emissions of castor biodiesel blends and Alumina nano additive blended castor biodiesel.

Smoke emission

Smoke emissions, primarily composed of soot particles resulting from incomplete combustion, generally increase as engine load rises from 0 to 100%. Diesel engines are particularly prone to higher smoke emissions compared to biodiesel and biodiesel blends because of differences in combustion characteristics and fuel properties. Diesel has fewer oxygen atoms and a larger carbon-to-hydrogen ratio, which results in incomplete combustion, especially during higher loads, and it emits more particulate matter and smoke[67]. Biodiesel and its blends usually emit less smoke than normal diesel because of their higher content of oxygen, which also improves complete combustion. This phenomenon is most pronounced in low engine loads. Here, oxygen present in biodiesel does the better oxidization of hydrocarbons and results in fewer soot particles. In turn, it reduces smoke exhaust. This cleaner combustion property of biodiesel makes visible emissions an environmental

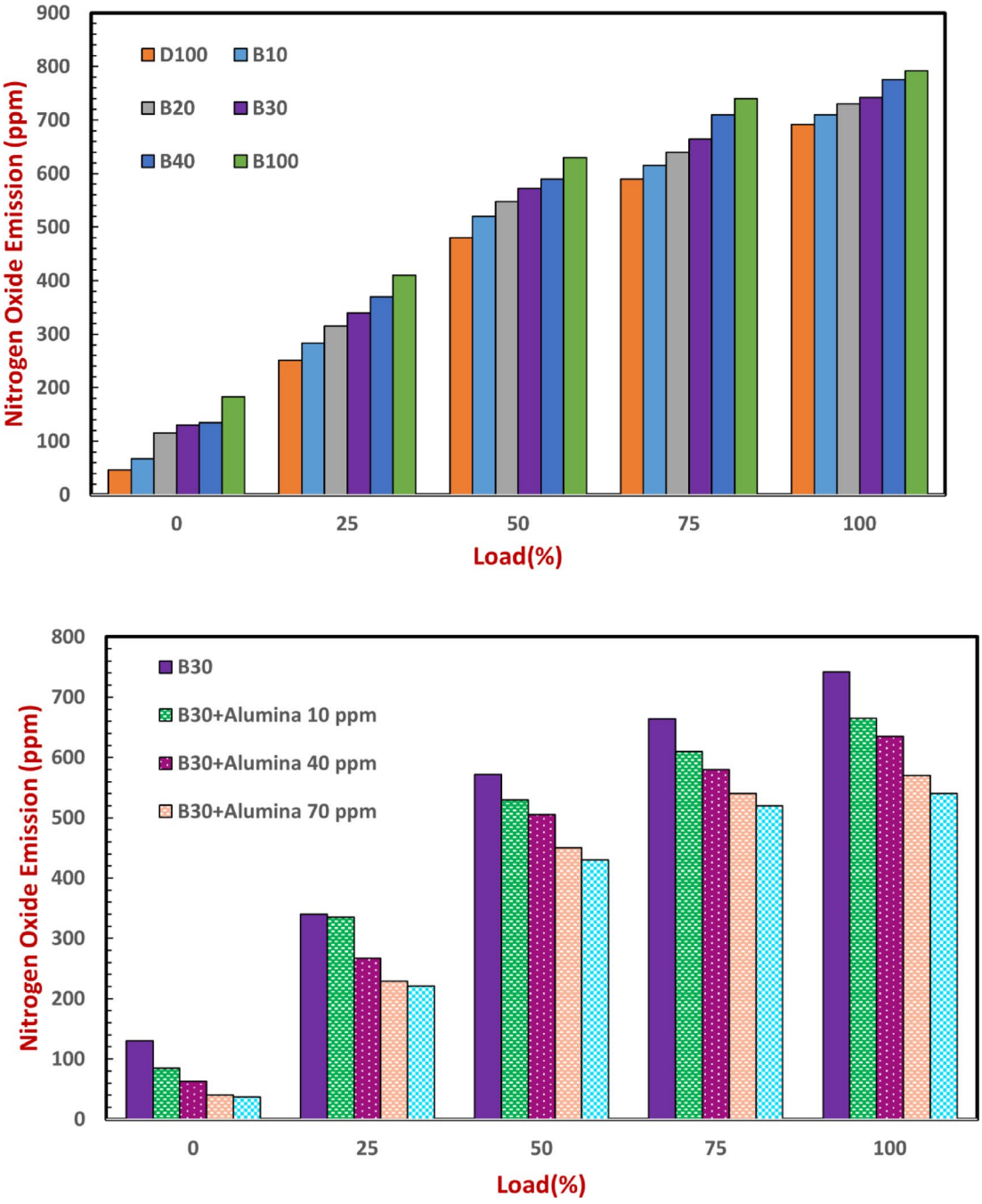

Fig. 6. NOx emissions of castor biodiesel blends and alumina nano additive blended castor biodiesel.

benefit of using biodiesel. A study found that adding alumina nanoparticles to a biodiesel blend reduced smoke opacity by 7.3%, further improving its emission profile[68]. Among various biodiesel blends, B30 strikes a balance between reducing emissions and maintaining combustion stability. B30 typically results in lower smoke emissions than neat biodiesel because the diesel content helps improve ignition characteristics, reducing the likelihood of incomplete combustion. Studies show that B30 outperforms both B10 and neat biodiesel in minimizing smoke emissions due to this blend's more efficient combustion processes[69]. The addition of alumina to B30 blends enhances this effect, with reductions becoming more pronounced as the concentration of alumina increases. A B30 biodiesel blend of alumina nanoparticles reduces the smoke emission greatly compared with a pure diesel and the higher alumina concentrations increase this improvement in smoke emission, resulting in 10 ppm at 28.30% for alumina, 33.96% for 40 ppm, 47.17% at 70 ppm, and 49.06% for 100 ppm. These results demonstrate the role of alumina nanoparticles in enhancing combustion efficiency, leading to better fuel burn and a dramatic reduction in smoke emissions. The trend illustrates how blends doped with alumina in biodiesel have a potential for a significant reduction of particulate emissions in diesel engines. These results indicate that the catalytic properties of alumina significantly enhance combustion efficiency, leading to a marked decrease in smoke emissions. Even when compared to neat biodiesel, B30 blends with alumina additives demonstrate superior performance in reducing smoke emissions. B30 with 10 ppm alumina reduces smoke emissions by 9.52% compared to B100, and this reduction grows to 16.67%, 33.33%, and 35.71% for alumina concentrations of 40 ppm, 70 ppm, and 100 ppm, respectively. This analysis highlights the effectiveness of alumina additives in further mitigating smoke emissions, even in blends that already exhibit lower emissions compared to pure diesel[70]. Figure 7 shows variations in Smoke emissions of Castor biodiesel blends and Alumina nano additive blended castor biodiesel.

Engine performance and emission data distribution

The histogram shows the distribution of engine load, pointing to both random and periodic peaks. These patterns help identify the conditions at which the engine operates optimally or sub-optimally[71]. The data suggests that the engine is optimized for certain load settings, though further testing is necessary to confirm why these specific settings are maintained. This information is crucial for optimizing load management and improving engine performance in real-world conditions. The histogram for BTE shows one prominent peak, especially between 0 and 30% load, indicating that the engine performs best at lower load levels. The largest peak near 0% suggests that the engine may be idle or under low-load conditions most of the time. This analysis could help identify the need for operational adjustments to improve efficiency during higher loads[72]. The BSFC histogram shows two significant peaks, around 0.3 and 0.5–0.6 kg/kW.hr. This irregularity could indicate fluctuations in fuel efficiency due to varying load conditions, fuel quality, or engine settings. Optimizing these conditions could help reduce fuel consumption and improve overall performance. CO emissions cluster between 0.05 and 0.25%, with HC emissions clustering around 20–40 and 60–80 ppm. These peaks highlight periods of incomplete combustion, suggesting that adjustments in fuel delivery, combustion temperature, or air–fuel mixture could improve combustion efficiency and reduce harmful emissions[73]. NOx emissions tend to peak around 100, 400–500, and 600–700 ppm, indicating the engine's sensitivity to load and temperature, which influence NOx formation. This finding underscores the importance of implementing NOx-reduction strategies, especially during high-load, high-temperature operations. The Smoke histogram, showing particulate emissions ranging from 10 to 50%, reflects the need for fuel type optimization and enhanced combustion efficiency to minimize particulate matter. The histograms demonstrate prominent peaks in engine performance and emission data for different load conditions. The histogram of Load (%) exhibits a peak at 100%, which shows frequent testing under full-load conditions. BTE (%) peaks at 27%, showing maximum combustion efficiency at average load conditions. BSFC peaks around 0.6 kg/kW.hr, which implies more fuel being consumed at very high loads. CO (%) is at a maximum of 0.1%, presumably a result of poor combustion at light loads, and HC (ppm) at a maximum of 40 ppm, the result of inferior fuel atomization. NOx (ppm) has its peak at 600 ppm due to elevated combustion temperatures and surplus oxygen at high loads. Finally, Smoke (%) at its maximum occurs at approximately 50%, signifying elevated particulate generation due to rich combustion conditions at heavy loads. Figure 8 shows the Histogram analysis of engine performance and emission parameters.

Correlation heat map

The correlation heatmap further unveils the strongest relationships of the engine performance and emission parameters among them, thereby leading to major insights in their interaction. Load (%) and Brake Thermal Efficiency (BTE%) have most of the other variables with which they are positively correlated, while they show a negative correlation with Brake Specific Fuel Consumption (BSFC). This clearly, therefore, shows that as the engine load and efficiency rise, a lower consumption of fuel per unit of power is attained[74]. This means both Load (%) and BTE (%) have a relatively strong inverse relationship with the BSFC (kg/kW.hr), signifying that as load and, consequently, the efficiency of the engine goes up, its fuel consumption goes down.

On the other hand, a negative strong correlation is exhibited between Carbon Monoxide (CO%), Hydrocarbons (HC ppm), and Smoke'%, meaning that the emissions would normally rise together. There is a strong positive correlation of the NOx ppm emissions with Load (%) and BTE (%), which implies that with an increase in engine load and efficiency, NOx formation increases. Again, the strong interrelationship between CO%, HC (ppm), and Smoke (%) suggests that there may be problems in reducing these simultaneously[75]. Overall, the heat map reiterates a web of such complicated trade-offs between engine performance and emissions, pointing out the importance of knowing such correlations for optimization of engine designing and operation to optimally balance performance with environmental impact. Figure 9 shows the corelation Heatmap analysis for performance and emission parameters.

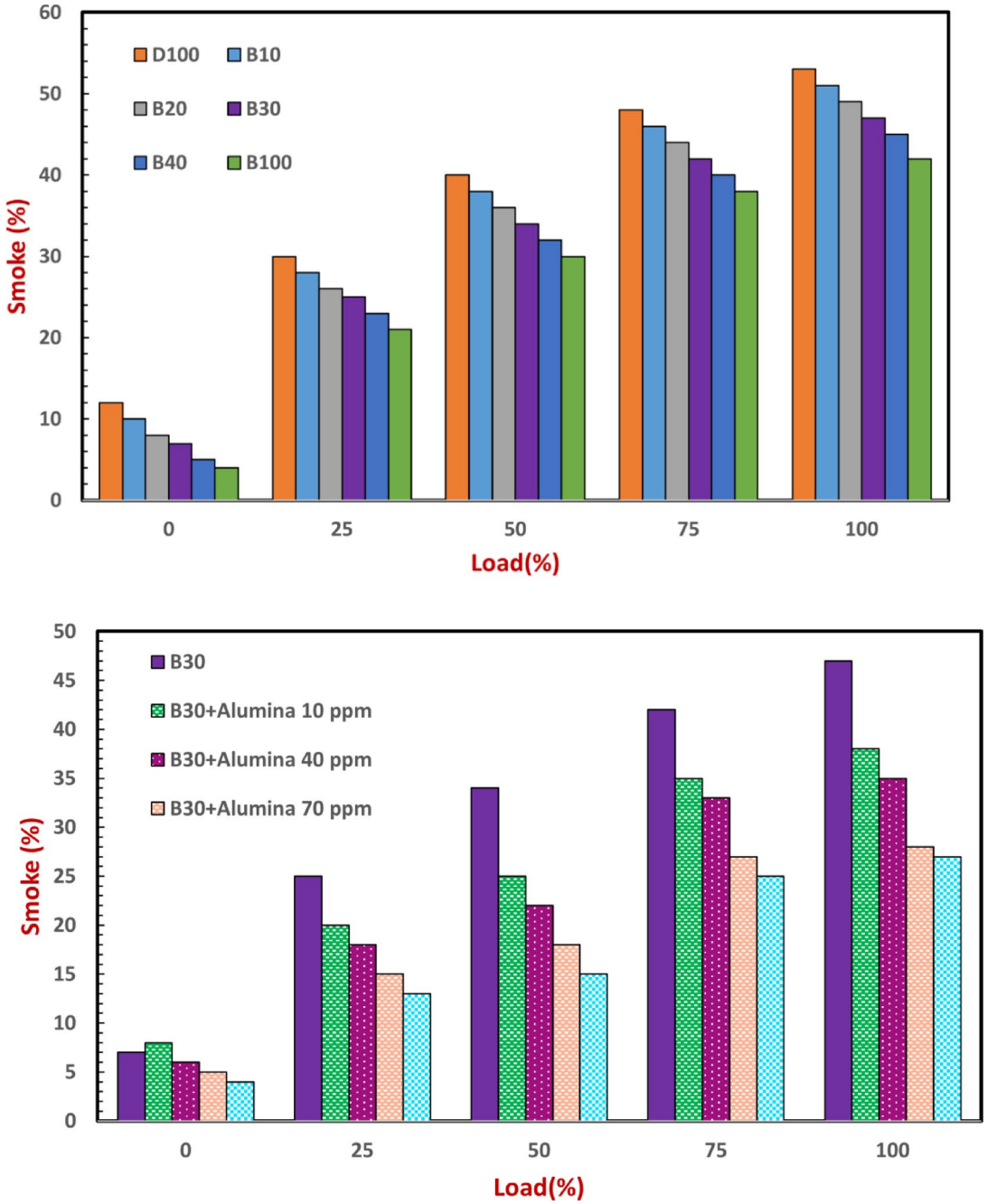

Fig. 7. Smoke emissions of castor biodiesel blends and alumina nano additive blended castor biodiesel.

Analysis of predicted versus measured values for random forest and XGBoost models

The basis for this study was to compare the performance of Random Forest and XGBoost models regarding their predictive capabilities in both engine performance and emission parameters. Model performances were assessed by plotting predicted values against measured values of BSFC and evaluating two crucial metrics: R-squared (R^2) used to indicate the variance explained by a model, and Root Mean Square Error (RMSE) to quantify the error involved in the prediction. Those two metrics are used to highlight the predictive reliability of such models and their potential application for accurate engine performance and emissions forecasting.

Prediction of brake specific fuel consumption

The BSFC prediction using the Random Forest model demonstrates a strong correlation between measured and predicted values, as evidenced by an R^2 value of 0.89 and an RMSE of 0.034 kg/kW.hr. This means that the model explains 89% of the variance in measured BSFC values, and suggests sufficiently correct predictions, though the presence of several outliers points out possible directions for improvement. To give a better comparison, the best

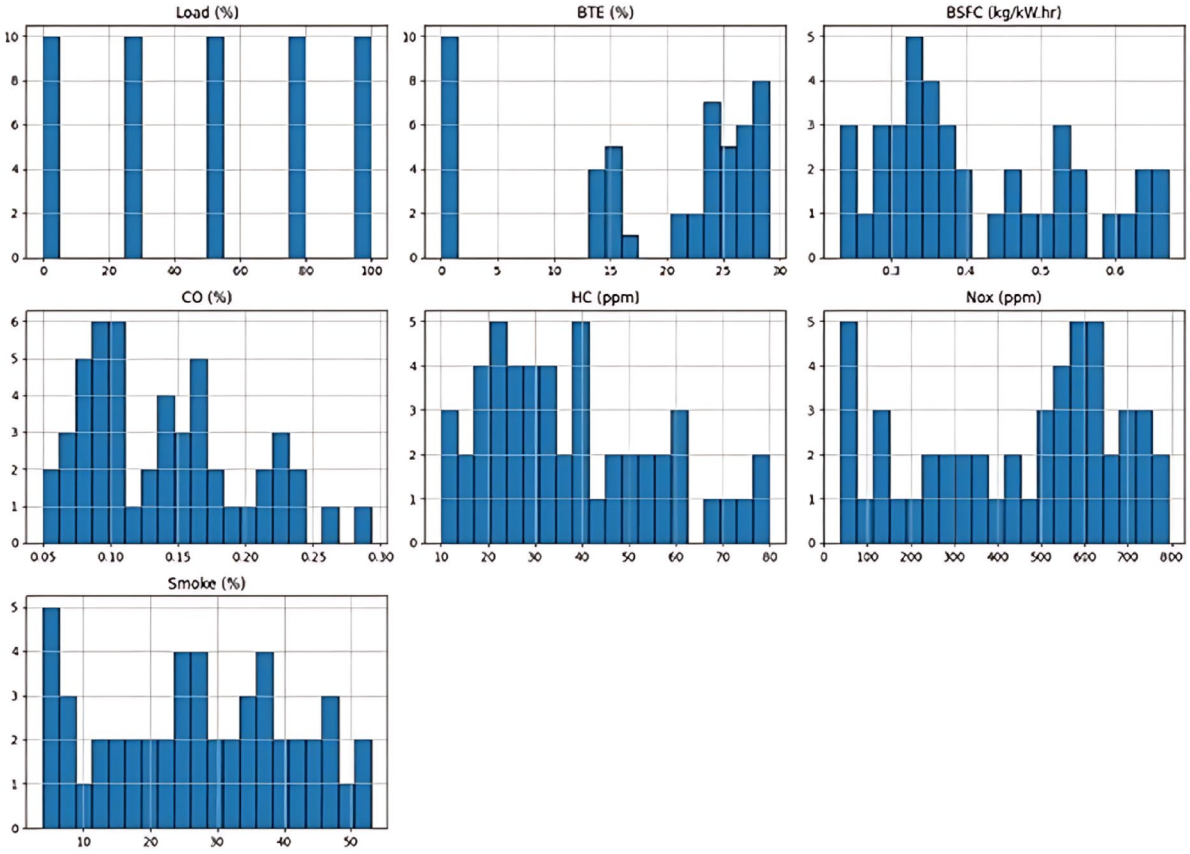

Fig. 8. Histogram analysis of engine performance and emission parameters.

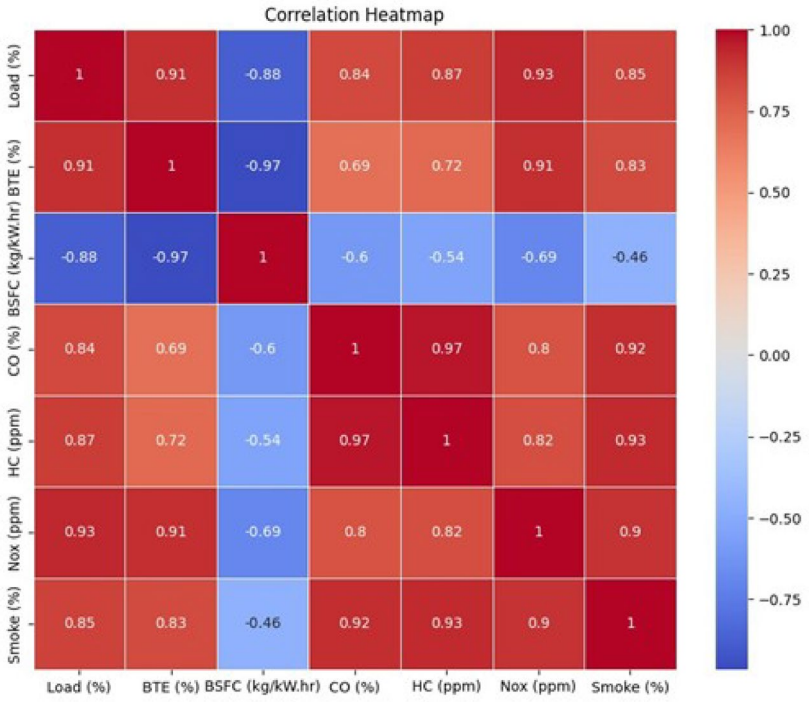

Fig. 9. Corelation heatmap analysis for performance and emission parameters.

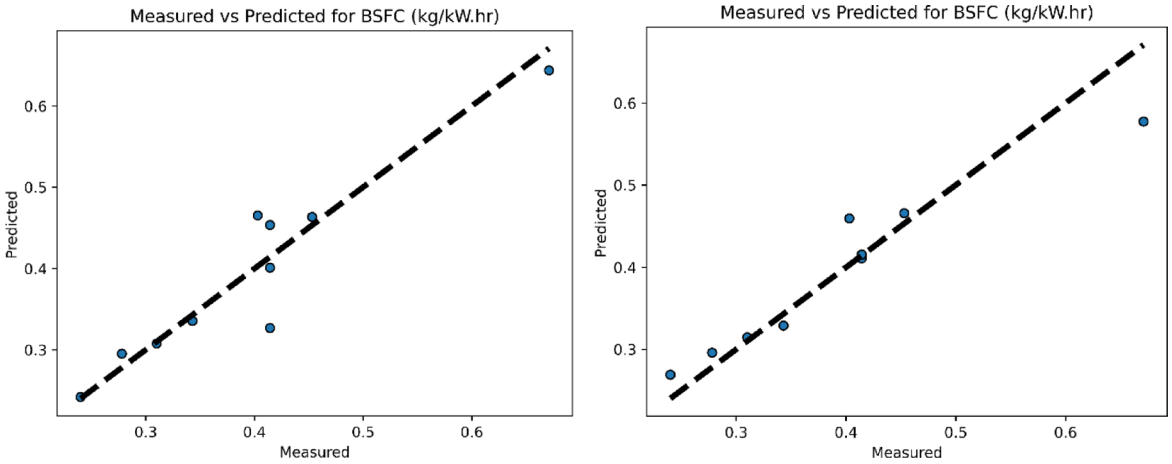

Fig. 10. Prediction of brake specific fuel consumption by XG boost and RF model.

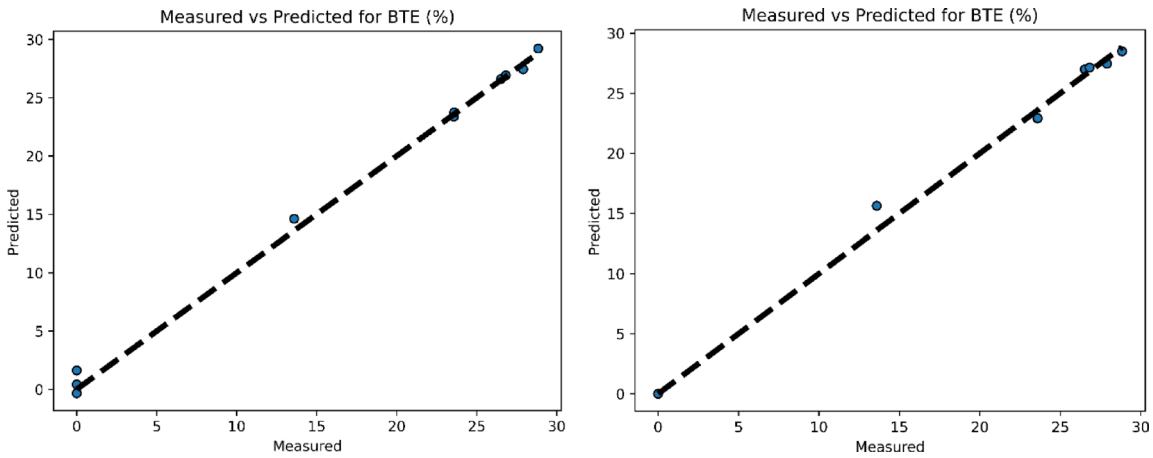

Fig. 11. Prediction of brake thermal efficiency by XG boost and RF model.

performing XGBoost model has an R^2 value of 0.91 and a RMSE value of 0.030 kg/kW.hr—this one accounts for 91% of variance and provides generally more accurate predictions on average[76]. Both models' scatter plots show that they follow the ideal fit line quite closely, meaning they are making predictions with higher accuracy. While both models are performing great, the XGBoost model is slightly more reliable, having a higher R^2 and a relatively lower RMSE[77]. What it essentially means is that the XGBoost model is slightly more reliable to be selected for the prediction of BSFC. However, the presence of the outliers for both models suggests an area for further improvement. These could be additional features that better capture the nuances of the data, using more advanced techniques of tuning to optimize parameters on the model, or just finding hybrid models that take a better approach combining both Random Forest and XGBoost. Handling these outliers is very important in aiding the improvement of accuracy and reliability of the models. In summary, both Random Forest and the XGBoost models are efficient at BSFC prediction, though the XGBoost model appears to be more promising with superior performance metrics. Though steady refinement and improvement are required to approach more accurate reliability in BSFC predictions, it would at least ensure the models could be utilized in practical applications without uncertainty. Figure 10 represents the prediction of Brake specific fuel consumption by XG boost and RF model.

Prediction of brake thermal efficiency

The predictive accuracy of the XGBoost model is excellent for the BTE, as seen in Fig. 11, and gives an R^2 value of 0.98, which means that 98% of the variance in the measured BTE values is accounted for by the model. The RMSE of 1.2% represents minimal prediction error, and most data points are very close to the ideal fit line, which means that the model can be described as accuracy. On the other hand, the Random Forest model as shown in Fig. 2 is strongly correlated at R^2 of 0.96 with an RMSE of 1.5%[78]. It's noticed that it produces predictions with less accuracy, but still, predictions by the Random Forest model are quite close to the ideal fit line. Both of the models possess great predictability abilities for BTE, but the XGBoost model has much larger R^2 high values and smaller RMSE values that indicate slightly better performance and more accurate predictions. The minor

increase in variance seen with the Random Forest model indicates areas where there is scope to enhance the model, for instance, introduction of more features or model parameter optimization[79]. Generally, both models are efficient however, the XGBoost model emerges as the best since it showed better accuracy with an error value during prediction close to zero, which essentially favours it in BTE prediction. The development of models is crucial to improve their predictive performances and accuracy so that they can be effectively used in practical applications. Figure 11 represents the prediction of Brake thermal efficiency by XG boost and RF model.

Prediction of CO emission

The model's ability to predict Carbon Monoxide (CO) has an R^2 of 0.95 in absolute value, which implies that the model explains 95% of the variance in measured CO values. A very low prediction error is indicated by the RMSE of 0.012, which shows how close the predictions are to the actual measured values and, therefore, the reliability of the model. Meanwhile, the Random Forest model is also very effective. Its resultant R^2 value was 0.93, which had a much stronger correlation between measured and predicted values, however at slightly lower levels as compared with the XGBoost model[80]. The RMSE for the Random Forest model was 0.015. Although this is higher than the RMSE from the XGBoost model, it is high in terms of accuracy. In sum, both are very strong predictors of CO emissions. However, the higher R^2 and lower RMSE of the XGBoost model give it marginally better performance and more reliable predictions than the Random Forest model. Thus, the XGBoost model should be more accurate and reliable in predicting CO emissions. However, the differences in the metrics of performance would imply that there are sections for improvement within the Random Forest model, such as feature selection or further tuning of model parameters, to better enhance predictability accuracy and reliability. Figure 12 represents the prediction of CO emission by XG boost and RF model.

Prediction of HC emission

For Hydrocarbons (HC), the XGBoost model predicts at good precision as shown in R^2 at 0.94, meaning that 94% of variance for measured HC values is captured in the model. RMSE at 3.5 ppm reflects minimal error from prediction and shows that the model was precise. The Random Forest model also performed well at an R^2 of 0.91, explaining 91% of variance for the measured HC values. The RMSE for this case is 4.0 ppm, which means that its predictions are not quite as precise as those of the XGBoost model. In the conclusion, it can be stated that both models have excellent predictive capabilities for HC emissions. The XGBoost model has a superior value for R^2 and significantly lower RMSE, making its predictions more accurate and reliable compared to the Random Forest model[81]. This means that while predicting HC emission, use of XGBoost is preferred because it exhibits better explanatory power and has a higher value for accuracy in predicting. In this respect, the performance of the model is still good for the Random Forest model since it may still be improved based on further selection of some features or through model tuning to improve its ability to predict further and become more reliable. Figure 13 represents the Prediction of HC emission by XG boost and RF model .

Prediction of NOx emission

High accuracy was indicated for the prediction of NOx by the XGBoost model, with a high R^2 value of 0.92, meaning that 92% variability in the measured NOx values is accounted for by the model. The RMSE of 28 ppm further established the precision towards predictions. In comparison, the model of Random Forest is similar with an R^2 of 0.90, which enables explaining 90% variability in NOx measured values[82]. However, the much larger value of its RMSE is 35 ppm, which shows that in comparison to the XGBoost model, the model makes predictions less accurately. In general, both models deliver great predictability on NOx emissions, while in comparison, the XGBoost model outperforms the Random Forest model because of a greater value of R^2 and smaller of RMSE value[83]. This suggests that the XGBoost model is giving more accurate and reliable predictions regarding NOx emissions. Although both models are robust, better metrics of the XGBoost model make it the first preferred choice in NOx prediction. Although the Random Forest model is effective, it does require further refinement and tuning so that its predictive accuracy is bettered and fewer errors are observed, which would

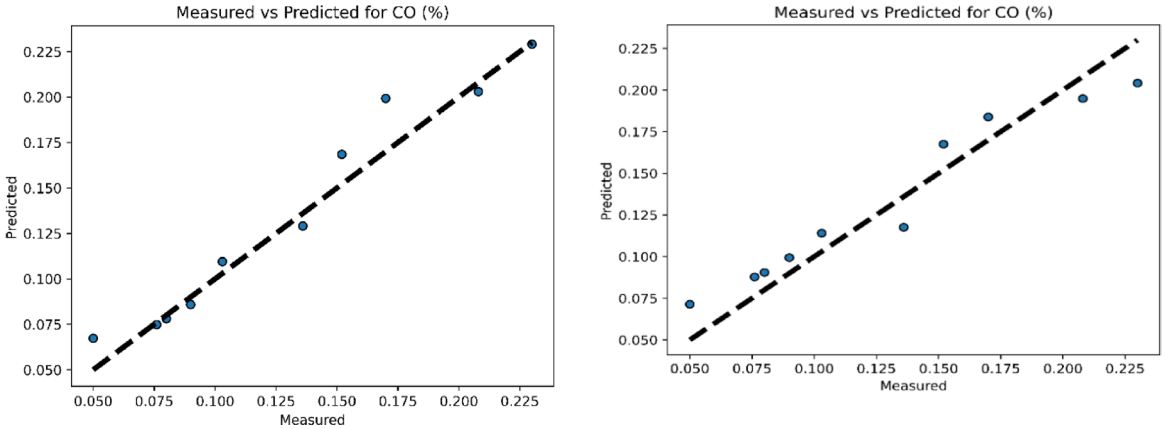

Fig. 12. Prediction of CO emission by XG boost and RF model.

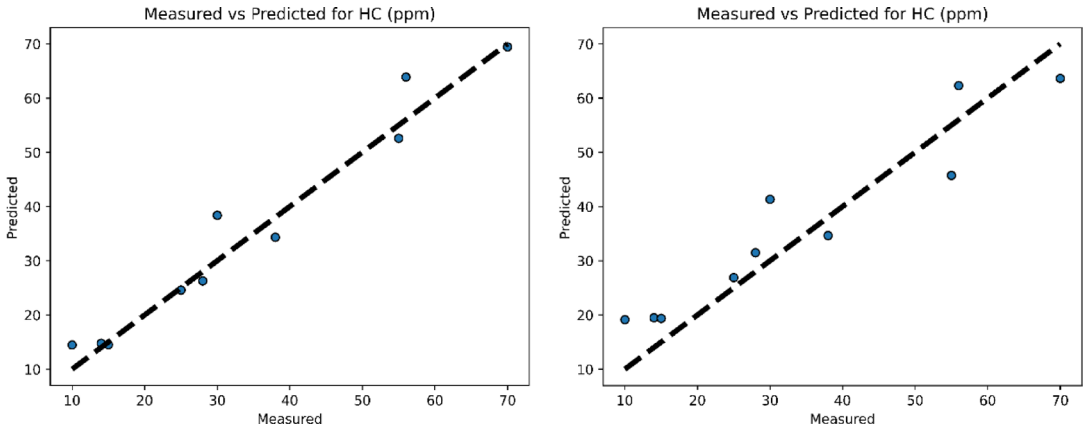

Fig. 13. Prediction of HC emission by XG boost and RF model.

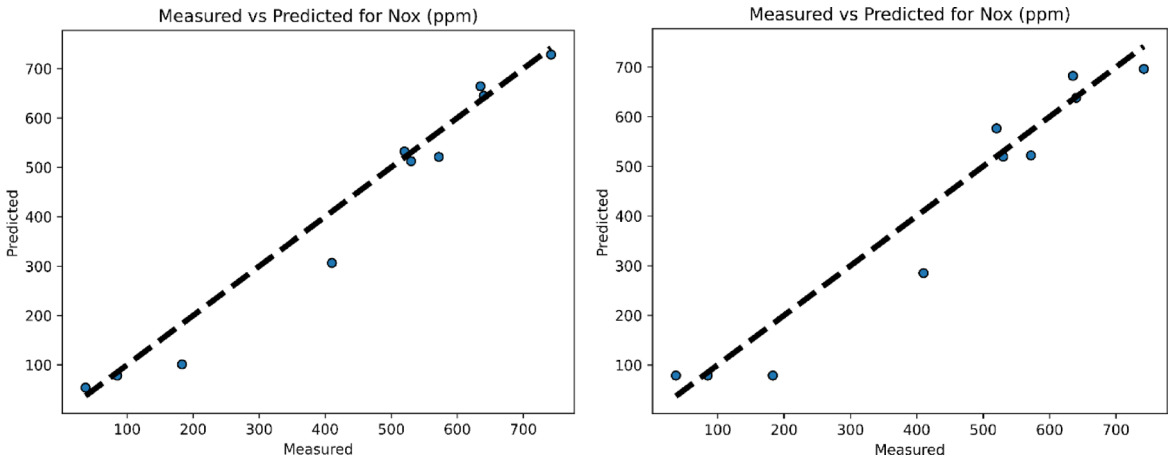

Fig. 14. Prediction of NOx emission by XG boost and RF model.

close the gap in respect of performance from that of the XGBoost model. Figure 14 represents the prediction of NOx emission by XG boost and RF model.

Prediction of smoke emission

The values of the predicted Smoke emissions in the XGBoost model were very close to each other, with an R^2 value of 0.96, that is, the model explains 96% variance in the measured Smoke values. A low RMSE of 1.8% further shows the keen accuracy of the model in making the predictions. The Random Forest model also performs similarly, with an R^2 value of 0.93, meaning it explains 93% of the variance in the measured Smoke values. Its RMSE of 2.2% suggests a bit less accurate prediction, though, compared with the XGBoost model. In short, both models strongly predict Smoke emissions. Also, R-Squared value of the XGBoost model is higher, and RMSE value is smaller compared to that of the Random Forest model, which is the accuracy and reliability of the prediction. Therefore, the superior metrics of the XGBoost model make it the preferable choice for prediction of Smoke emissions. Even though the performances of the two models are strong, a slight gap between the two models indicates that there is still further refinement area that may need to be done in the Random Forest model, for example, improvement of feature selection or the model parameter optimization to adjust the high predicting power of this model to close the gap with the XGBoost model[79]. Figure 15 represents the prediction of smoke emission by XG boost and RF model. Table 4 shoes the comparison of the current study with previous results.

Conclusion

- The incorporation of aluminum oxide nano-additives into B30 biodiesel blends significantly improves engine performance and reduces environmental emissions, making it a viable strategy for cleaner combustion.
- Experimental results show CO emissions reduced by 25%, HC emissions by 20%, smoke emissions by 15%, and NOx emissions by 10%, mainly due to improved atomization, fuel–air mixing, and catalytic activity of aluminum oxide.

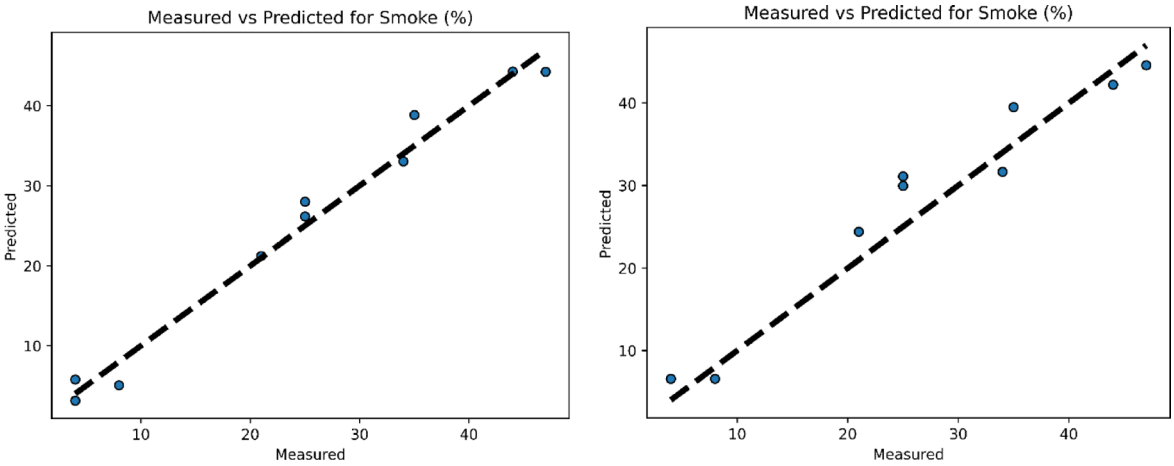

Fig. 15. Prediction of smoke emission by XG boost and RF model.

Parameters	Present study	Nibin et al. 2021[58]	Thiyagarajan et al. 2020[75]	Soloiu et al. 2018[61]
BTE	4.12% ↓	2.14% ↓	6.06% ↓	2% ↓
BSFC	4.28% ↑	2% ↑	4.83% ↓	1.8% ↓
NOx	75% ↓	10% ↓	22% ↓	15% ↓
Smoke	45% ↓	15% ↓	7.06% ↓	84% ↓
HC	3.33% ↓	6.25% ↑	80% ↑	12% ↑
CO	3.27% ↓	7.14% ↑	24.83% ↑	5% ↑

Table 4. A comparison of the current study with previous results.

- Performance gains include a 3% increase in brake thermal efficiency (BTE) and a 4% reduction in brake-specific fuel consumption (BSFC), indicating better energy utilization.
- The correlation heatmap highlights key relationships between engine performance and emissions, aiding in optimizing engine design for a balance between efficiency and environmental impact.
- Random Forest (RF) and XGBoost models were used to predict engine parameters, with XGBoost showing superior performance, achieving $R^2 = 0.91$ for BSFC, $R^2 = 0.98$ for BTE, and lower RMSE values, making it more reliable.
- In CO emissions prediction, XGBoost explains 95% variance ($R^2 = 0.95$) with lower RMSE than RF ($R^2 = 0.93$), indicating higher accuracy and better correlation with measured values.
- For HC emissions, XGBoost achieves $R^2 = 0.94$, while RF explains 91% variance, but RF requires further tuning to improve predictive reliability.
- NOx emissions prediction shows XGBoost ($R^2 = 0.92$) outperforming RF ($R^2 = 0.90$), as RF had a higher RMSE (35 ppm), making XGBoost the preferred choice for accuracy.
- Smoke emissions were strongly predicted, with XGBoost explaining 96% variance and achieving a low RMSE of 1.8%, but RF requires further refinement for better performance.
- Challenges include outliers affecting predictive accuracy, potential overfitting in XGBoost, and the need for hybrid modeling strategies to enhance reliability and generalizability.
- Future work should focus on long-term durability and stability studies, tribological analysis, and testing non-metallic nano-additives to explore their impact on engine wear, emissions, and fuel efficiency.
- While XGBoost is the superior model, further feature selection, model tuning, and deep learning integration could improve predictive accuracy and optimize nano-additive blended biodiesel performance for real-world applications[84].

Data availability

The datasets used and/or analysed during the current study available from the corresponding author on reasonable request.

Received: 9 January 2025; Accepted: 13 May 2025
Published online: 21 October 2025

References

1. Emma, A. F., Alangar, S. & Yadav, A. K. Extraction and characterization of coffee husk biodiesel and investigation of its effect on performance, combustion, and emission characteristics in a diesel engine. *Energy Convers. Manag. X* **14**(January), 100214. https://doi.org/10.1016/j.ecmx.2022.100214 (2022).
2. Gautam, R. & Kumar, S. Performance and combustion analysis of diesel and tallow biodiesel in CI engine. *Energy Rep.* **6**, 2785–2793. https://doi.org/10.1016/j.egyr.2020.09.039 (2020).
3. Jain, A., Yadav, A. K., Mallick, P., Yadav, S. N. & Kumar, N. Estimation of the potential of Nahar biodiesel run diesel engine at varying fuel injection pressures and engine loads through exergy approach. *Alex. Eng. J.* **84**(February), 262–274. https://doi.org/10.1016/j.aej.2023.11.014 (2023).
4. Rao, B. N., Kumar, M., Kumar, A. S. & Dinesh, D. Utilization of additives in biodiesel blends for improving the diesel engine performance and minimizing emissions through a modified Taguchi approach. *Heliyon* **9**(6), e16950. https://doi.org/10.1016/j.heliyon.2023.e16950 (2023).
5. Mofijur, M., Ong, H. C., Saidur, R. & Rasul, M. G. Impact of nanoparticle-based fuel additives on biodiesel combustion: An analysis of fuel properties, engine performance, emissions, and combustion characteristics. *Energy Convers. Manag. X* **21**(November), 100515. https://doi.org/10.1016/j.ecmx.2023.100515 (2023).
6. Sayyed, S., Das, R. K., Kulkarni, K., Alam, T. & Eldin, S. M. Influence of additive mixed ethanol-biodiesel blends on diesel engine characteristics. *Alex. Eng. J.* **71**, 619–629. https://doi.org/10.1016/j.aej.2023.03.091 (2023).
7. Leach, F., Kalghatgi, G., Stone, R. & Miles, P. The scope for improving the efficiency and environmental impact of internal combustion engines. *Transp. Eng.* **1**(May), 100005. https://doi.org/10.1016/j.treng.2020.100005 (2020).
8. Sarma, C. J., Khond, B. S., Deb, M. & Nandi, G. Improving the combustion and emission performance of a diesel engine powered with mahua biodiesel and TiO_2 nanoparticles additive. *Alex. Eng. J.* **72**, 387–398. https://doi.org/10.1016/j.aej.2023.03.070 (2023).
9. Anwar, F., Tariq, M., Nisar, J., Ali, G. & Kanwal, H. Optimization of biodiesel yield from non-food karanja seed oil: Characterization and assessment of fuel properties. *Sustain. Chem. Environ.* **3**(July), 100035. https://doi.org/10.1016/j.scenv.2023.100035 (2023).
10. Rana, R. P. & Dahiya, V. Life cycle assessment of biodiesel production from waste cooking oil. *J. Clean. Prod.* **14**(August), 100850. https://doi.org/10.1016/j.envc.2024.100850 (2021).
11. Nurmukan, D., Tran, M.-V., Hung, Y. M., Scribano, G. & Chong, C. T. Effect of multi-walled carbon nanotubes on pre-vaporized palm oil biodiesel/air premixed flames. *Fuel Commun.* **8**, 100020. https://doi.org/10.1016/j.jfueco.2021.100020 (2021).
12. Lamore, M. T., Zeleke, D. S. & Kassa, B. Y. A comparative study on the effect of nano-additives on performance and emission characteristics of CI engine run on castor biodiesel blended fuel. *Energy Convers. Manag. X* **20**(November), 100493. https://doi.org/10.1016/j.ecmx.2023.100493 (2023).
13. Mujtaba, M. A., Masjuki, H. H., Kalam, M. A., Shahabuddin, M. & Varman, M. Effect of alcoholic and nano-particles additives on tribological properties of diesel–palm–sesame–biodiesel blends. *Energy Rep.* **7**, 1162–1171. https://doi.org/10.1016/j.egyr.2020.12.009 (2021).
14. Karami, S. & Gharehghani, A. Effect of nano-particles concentrations on the energy and exergy efficiency improvement of indirect-injection diesel engine. *Energy Rep.* **7**, 3273–3285. https://doi.org/10.1016/j.egyr.2021.05.050 (2021).
15. Razzaq, L., Rahman, M. K. U., Rafique, K. M. & Nadeem, M. Influence of varying concentrations of TiO_2 nanoparticles and engine speed on the performance and emissions of diesel engine operated on waste cooking oil biodiesel blends using response surface methodology. *Heliyon* **9**(7), e17758. https://doi.org/10.1016/j.heliyon.2023.e17758 (2023).
16. Gavhane, R. S., Kumar, S., Patel, A. K. & Sahoo, A. R. Effect of zinc oxide nano-additives and soybean biodiesel at varying loads and compression ratios on VCR diesel engine characteristics. *Symmetry* **12**(6), 1042. https://doi.org/10.3390/sym12061042 (2020).
17. Gharehghani, A. & Pourrahmani, H. Performance evaluation of diesel engines (PEDE) for a diesel-biodiesel fueled CI engine using nano-particles additive. *Energy Convers. Manag.* **198**, 111921. https://doi.org/10.1016/j.enconman.2019.111921 (2019).
18. Mehregan, M. & Moghiman, M. Effects of nano-additives on pollutants emission and engine performance in a urea-SCR equipped diesel engine fueled with blended-biodiesel. *Fuel* **222**, 402–406. https://doi.org/10.1016/j.fuel.2018.02.172 (2018).
19. Chacko, N. & Jeyaseelan, T. Comparative evaluation of graphene oxide and graphene nanoplatelets as fuel additives on the combustion and emission characteristics of a diesel engine fuelled with diesel and biodiesel blend. *Fuel Process. Technol.* **204**, 106406. https://doi.org/10.1016/j.fuproc.2020.106406 (2020).
20. Sheriff, S. A., Ganesh, A. R., Sahu, A. K. & Raj, P. P. Emission reduction in CI engine using biofuel reformulation strategies through nano additives for atmospheric air quality improvement. *Renew. Energy* **147**, 2295–2308. https://doi.org/10.1016/j.renene.2019.10.041 (2020).
21. Soji-Adekunle, A. R. et al. Optimization and modeling of the performance of compression ignition engine fired on biofuel from non-edible vegetable oils. *Clean. Energy Syst.* **7**(August), 100105. https://doi.org/10.1016/j.cles.2023.100105 (2024).
22. Rao, P. M., Nagarajan, S., Kumar, K. & Veera, S. Artificial intelligence-based modeling and hybrid optimization of linseed oil biodiesel with graphene nanoparticles to stringent biomedical safety and environmental standards. *Case Stud. Therm. Eng.* **51**(April), 103554. https://doi.org/10.1016/j.csite.2023.103554 (2023).
23. Seela, C. R., Ravisankar, B. & Raju, B. M. V. A. A GRNN-based framework to test the influence of nano zinc additive biodiesel blends on CI engine performance and emissions. *Egypt. J. Pet.* **27**(4), 641–647. https://doi.org/10.1016/j.ejpe.2017.09.006 (2018).
24. Ghanbari, M., Mozafari-Vanani, L., Dehghani-Soufi, M. & Jahanbakhshi, A. Effect of alumina nanoparticles as additive with diesel–biodiesel blends on performance and emission characteristic of a six-cylinder diesel engine using response surface methodology (RSM). *Energy Convers. Manag. X* **11**, 100091. https://doi.org/10.1016/j.ecmx.2021.100091 (2021).
25. Vellaiyan, S. Optimization of plastic waste pyrolysis using carbon-metal oxide hybrid nanocomposite catalyst: Yield enhancement and energy resource potential. *Results Eng.* **23**, 102520. https://doi.org/10.1016/j.rineng.2024.102520 (2024).
26. Sharma, V., Hossain, A. K., Ahmed, A. & Rezk, A. Study on using graphene and graphite nanoparticles as fuel additives in waste cooking oil biodiesel. *Fuel* **328**(June), 125270. https://doi.org/10.1016/j.fuel.2022.125270 (2022).
27. Raja, S., Kumar, M. S., Natarajan, S., Eshwar, D. & Alphin, M. S. Energy and exergy analysis and multi-objective optimization of a biodiesel-fueled direct ignition engine. *Results Chem.* **4**(August), 100284. https://doi.org/10.1016/j.rechem.2022.100284 (2022).
28. Taheri-Garavand, A., Heidari-Maleni, A., Mesri-Gundoshmian, T. & Samuel, O. D. Application of artificial neural networks for the prediction of performance and exhaust emissions in IC engine using biodiesel-diesel blends containing quantum dot-based carbon doped. *Energy Convers. Manag. X* **16**(May), 100304. https://doi.org/10.1016/j.ecmx.2022.100304 (2022).
29. Chen, Y. et al. Machine learning-based design of target property-oriented fuels using explainable artificial intelligence. *Energy* https://doi.org/10.1016/j.energy.2024.131583 (2024).
30. Sonawane, S., Sekhar, R., Warke, A., Thipse, S. & Varma, C. Forecasting of engine performance for gasoline-ethanol blends using machine learning. *J. Eng. Technol. Sci.* **55**(3), 340–355. https://doi.org/10.5614/J.ENG.TECHNOL.SCI.2023.55.3.10 (2023).
31. Badra, J., Owoyele, O., Pa, P. & Som, S. A machine learning-genetic algorithm approach for rapid optimization of internal combustion engines. In *Artificial Intelligence and Data-Driven Optimization of Internal Combustion Engines*, 125–158. https://doi.org/10.1016/B978-0-323-88457-0.00003-5 (2022).
32. Patel, K. R. & Dhiman, V. D. Effect of hybrid nanoparticles MgO and Al2O3 added water-in-diesel emulsion fueled diesel engine using hybrid deep neural network-based spotted hyena optimization. *Heat Trans.* **51**(6), 5748–5788. https://doi.org/10.1002/HTJ.22568 (2022).
33. Khan, O., Hussain, F., Haq, A., Shahzad, S. & Farooq, U. Modelling of compression ignition engine by soft computing techniques (ANFIS-NSGA-II and RSM) to enhance the performance characteristics for leachate blends with nano-additives. *Sci. Rep.* **13**(1), 15429. https://doi.org/10.1038/s41598-023-42353-1 (2023).

34. Meneghetti, S. M. P. et al. Biodiesel from castor oil: A comparison of ethanolysis versus methanolysis. *Energy Fuels* **20**(5), 2262–2265. https://doi.org/10.1021/ef060118m (2006).
35. Keera, S. T., El Sabagh, S. M. & Taman, A. R. Castor oil biodiesel production and optimization. *Egypt. J. Pet.* **27**(4), 979–984. https://doi.org/10.1016/j.ejpe.2018.02.007 (2018).
36. Sharma, P., Paramasivam, P., Bora, B. J. & Sivasundar, V. Application of nanomaterials for emission reduction from diesel engines powered with waste cooking oil biodiesel. *Int. J. Low-Carbon Technol.* **18**, 795–801. https://doi.org/10.1093/ijlct/ctad060 (2023).
37. Kumar, V. D., Rajendran, S., Hemadri, V. B., Prakash, C. & Saravanakumar, S. Experimental investigation of operating parameter effect on DI CI diesel engine using flamboyant biodiesel blends. *Key Eng. Mater.* **1006**, 33–42. https://doi.org/10.4028/p-j7hz6w (2024).
38. Alotaibi, J. G., Alajmi, A. E., Alsaeed, T., Al-lwayzy, S. H. & Yousif, B. F. On the influence of engine compression ratio on diesel engine performance and emission fueled with biodiesel extracted from waste cooking oil. *Energies* **17**(15), 3844. https://doi.org/10.3390/en17153844 (2024).
39. Yildizhan, S., Uludamar, E., Ozcanli, M., & Serin, H. Evaluation of effects of compression ratio on performance, combustion, emission, noise and vibration characteristics of a VCR diesel engine. *Int. J. Renew. Energy Res.* **8**(1), 90–100. https://ijrer.org/ijrer/index.php/ijrer/article/view/6573 (2018)
40. Guo, H. Transient lubrication of floating bush coupled with dynamics and kinematics of cam-roller in fuel supply mechanism of diesel engine. *Phys. Fluids* **36**(12), 123103. https://doi.org/10.1063/5.0232226 (2024).
41. Ji, C. Research on an integrated index prediction model based on RF-XGBOOST-ANN. In *Proceedings of the 2023 IEEE International Conference on Control, Electronics and Computer Technology (ICCECT)*, 545–549. https://doi.org/10.1109/ICCECT57938.2023.10140383 (2023).
42. Hassan, M. A., Salem, H., Bailek, N. & Kisi, O. Random forest ensemble-based predictions of on-road vehicular emissions and fuel consumption in developing urban areas. *Sustainability* **15**(2), 1–22 (2023).
43. Sanjeevannavar, M. B. et al. Machine learning prediction and optimization of performance and emissions characteristics of IC engine. *Sustainability* **15**(18), 13825. https://doi.org/10.3390/su151813825 (2023).
44. Breiman, L. Random forests. *Mach. Learn.* **45**(1), 5–32. https://doi.org/10.1023/A:1010933404324 (2001).
45. Chen, T. & Guestrin, C. XGBoost: A scalable tree boosting system. In *Proceedings of the 22nd ACM SIGKDD International Conference on Knowledge Discovery and Data Mining (KDD '16)*, 785–794. https://doi.org/10.1145/2939672.2939785 (2016).
46. Mohan, S. & Dinesha, P. Performance and emissions of biodiesel engine with hydrogen peroxide emulsification and cerium oxide (CeO_2) nanoparticle additives. *Fuel* **319**, 123872. https://doi.org/10.1016/j.fuel.2022.123872 (2022).
47. Paramasivam, P. et al. Exploring alternative fuel solutions: Lemon grass oil biodiesel blend with dibutyl ether additive for VCR diesel engines—An experimental analysis. *Sci. Rep.* **14**, 20272. https://doi.org/10.1038/s41598-024-70491-7 (2024).
48. Haryono, I. et al. An investigation of 30% palm biodiesel blend fuel (B30) under Indonesian operating conditions. *J. Oil Palm Res.* https://doi.org/10.21894/jopr.2024.0013 (2024).
49. Vellaiyan, S. Experimental study on energy and environmental impacts of alcohol-blended water emulsified cottonseed oil biodiesel in diesel engines. *Results Eng* **24**, 102873. https://doi.org/10.1016/j.rineng.2024.102873 (2024).
50. Kandasamy, A. & Jabaraj, D. B. Performance and emission characteristics of CI engine using diesel and biodiesel (Pongamia) blends with aluminum oxide nanoparticles as additive. *Int. J. Veh. Struct. Syst.* **9**(4), 148–153. https://doi.org/10.4273/ijvss.9.4.02 (2017).
51. Murugesan, A., Avinash, A., Gunasekaran, E. & Murugaganesan, A. Multivariate analysis of nano additives on biodiesel fuelled engine characteristics. *Fuel* **275**, 117922. https://doi.org/10.1016/j.fuel.2020.117922 (2020).
52. Jaikumar, S., Srinivas, V. & Rajasekhar, M. Influence of dispersant added nanoparticle additives with diesel-biodiesel blend on direct injection compression ignition engine: Combustion, engine performance, and exhaust emissions approach. *Energy* **224**, 120197. https://doi.org/10.1016/j.energy.2021.120197 (2021).
53. Elsharkawy, E., Abou Al-Sood, M. M. A., El-Fakharany, M. & Ahmed, M. Enhancing the impact of biodiesel blend on combustion, emissions, and performance of DI diesel engine. *Arab. J. Sci. Eng.* **45**, 1109–1123. https://doi.org/10.1007/s13369-019-04245-3 (2020).
54. Prabu, M. Nanoparticles as additive in biodiesel on the working characteristics of a DI diesel engine. *Ain Shams Eng. J.* https://doi.org/10.1016/j.asej.2017.04.004 (2017).
55. Fayaz, H. et al. Collective effect of ternary nano fuel blends on the diesel engine performance and emissions characteristics. *Fuel* https://doi.org/10.1016/j.fuel.2021.120420 (2021).
56. Nguyen, V. H. & Pham, P. X. Biodiesels: Oxidizing enhancers to improve CI engine performance and emission quality. *Fuel* **154**, 293–300. https://doi.org/10.1016/j.fuel.2015.04.004 (2015).
57. Mwangi, J. K., Lee, W. J., Chang, Y. C., Chen, C. Y. & Wang, L. C. An overview: Energy saving and pollution reduction by using green fuel blends in diesel engines. *Appl. Energy* **159**, 214–236. https://doi.org/10.1016/j.apenergy.2015.08.084 (2015).
58. Vedaraman, N., Puhan, S., Nagarajan, G. & Velappan, K. C. Preparation of palm oil biodiesel and effect of various additives on NOx emission reduction in B20: An experimental study. *Int. J. Green Energy* **8**(3), 383–397. https://doi.org/10.1080/15435075.2011.557847 (2011).
59. Mirzajanzadeh, M. et al. A novel soluble nano-catalysts in diesel–biodiesel fuel blends to improve diesel engines performance and reduce exhaust emissions. *Fuel* **139**, 374–382. https://doi.org/10.1016/j.fuel.2014.09.008 (2014).
60. Özener, O., Yüksek, L., Ergenç, A. T. & Özkan, M. Effects of soybean biodiesel on a DI diesel engine performance, emission and combustion characteristics. *Fuel* **115**, 875–883. https://doi.org/10.1016/j.fuel.2012.10.081 (2012).
61. Hussain, F. et al. Enhancement in combustion, performance, and emission characteristics of a diesel engine fueled with Ce-ZnO nanoparticle additive added to soybean biodiesel blends. *Energies* **13**(17), 4578. https://doi.org/10.3390/en13174578 (2020).
62. Gumus, S., Ozcan, H., Ozbey, M. & Topaloglu, B. Aluminum oxide and copper oxide nanodiesel fuel properties and usage in a compression ignition engine. *Fuel* **163**, 80–87. https://doi.org/10.1016/j.fuel.2015.09.048 (2015).
63. Nema, V. & Singh, A. Emission reduction in a dual blend biodiesel fuelled CI engine using nano-fuel additives. *Mater. Today Proc.* **5**, 20754–20759 (2018).
64. Chen, L. et al. Impacts of fuel stage ratio on the morphological and nanostructural characteristics of soot emissions from a Twin Annular Premixing Swirler combustor. *Environ. Sci. Technol.* **58**(24), 10558–10566. https://doi.org/10.1021/acs.est.4c03478 (2024).
65. Anchupogu, P., Rao, L. & Banavathu, B. Effect of alumina nano additives into biodiesel-diesel blends on the combustion performance and emission characteristics of a diesel engine with exhaust gas recirculation. *Environ. Sci. Pollut. Res.* **25**, 23294–23306. https://doi.org/10.1007/s11356-018-2366-7 (2018).
66. Hosseini, S. H., Taghizadeh-Alisaraei, A., Ghobadian, B. & Abbaszadeh-Mayvan, A. Effect of added alumina as nano-catalyst to diesel-biodiesel blends on performance and emission characteristics of CI engine. *Energy* **124**, 543–552. https://doi.org/10.1016/j.energy.2017.02.109 (2017).
67. Prabu, A. & Anand, R. Emission control strategy by adding alumina and cerium oxide nano particle in biodiesel. *J. Energy Inst.* **89**, 366–372. https://doi.org/10.1016/j.joei.2015.03.003 (2016).
68. Vellaiyan, S. Optimization of water and 1-pentanol concentrations in biodiesel-diesel blends for enhanced engine performance and environmental sustainability. *Results Eng.* **24**, 102953. https://doi.org/10.1016/j.rineng.2024.102953 (2024).
69. El-Seesy, A. I., Attia, A. & El-Batsh, H. The effect of aluminum oxide nanoparticles addition with Jojoba methyl ester-diesel fuel blend on a diesel engine performance, combustion and emission characteristics. *Fuel* **233**, 344–354. https://doi.org/10.1016/j.fuel.2018.03.076 (2018).

70. Gurusala, N. K. & Selvan, V. Effects of alumina nanoparticles in waste chicken fat biodiesel on the operating characteristics of a compression ignition engine. *Clean Technol. Environ. Policy* **17**, 681–692. https://doi.org/10.1007/s10098-014-0825-5 (2015).
71. Dhingra, S., Bhushan, G. & Dubey, K. Multi-objective optimization of combustion, performance and emission parameters in a jatropha biodiesel engine using non-dominated sorting genetic algorithm-II. *Front. Mech. Eng.* **9**, 81–94. https://doi.org/10.1007/s11465-014-0287-9 (2014).
72. Esonye, C., Onukwuli, O., Ofoefule, A. & Ogah, E. Multi-input multi-output (MIMO) ANN and Nelder-Mead's simplex-based modeling of engine performance and combustion emission characteristics of biodiesel-diesel blend in CI diesel engine. *Appl. Therm. Eng.* https://doi.org/10.1016/j.applthermaleng.2019.01.101 (2019).
73. Uslu, S. & Çelik, M. B. Prediction of engine emissions and performance with artificial neural networks in a single cylinder diesel engine using diethyl ether. *Eng. Sci. Technol. Int. J.* https://doi.org/10.1016/j.jestch.2018.08.017 (2018).
74. Beeravelli, V. N., Chanamala, R., Rayavarapu, U. M. R. & Kancherla, P. An artificial neural network and Taguchi integrated approach to the optimization of performance and emissions of direct injection diesel engine. *EJOSDR* https://doi.org/10.20897/EJOSDR/85412 (2018).
75. Singh, V. B. & Yadav, A. Optimisation of performance and emission characteristics of CI engine fuelled with Mahua oil methyl ester–diesel blend using response surface methodology. *Int. J. Ambient Energy* **41**, 674–685. https://doi.org/10.1080/01430750.2018.1484804 (2018).
76. Song, Y. et al. Cyclic coupling and working characteristics analysis of a novel combined cycle engine concept for aviation applications. *Energy* **301**, 131747. https://doi.org/10.1016/j.energy.2024.131747 (2024).
77. Zhang, X. et al. Hybrid triboelectric-variable reluctance generator assisted wireless intelligent condition monitoring of aero-engine main bearings. *Nano Energy* **136**, 110721. https://doi.org/10.1016/j.nanoen.2025.110721 (2025).
78. Gu, Z., Cao, M., Wang, C., Yu, N. & Qing, H. Research on mining maximum subsidence prediction based on genetic algorithm combined with XGBoost model. *Sustainability* https://doi.org/10.3390/su141610421 (2022).
79. Wan, A. et al. Aeroengine life prediction and status evaluation based on sequential multitask learning and health indicators. *IEEE Trans. Reliab.* 1–14. https://doi.org/10.1109/TR.2025.3535716 (2025).
80. Qiu, Z., Chen, R., Gan, X. & Wu, C. Torsional damper design for diesel engine: theory and application. *Physica Scripta* **99**(12), 125214. https://doi.org/10.1088/1402-4896/ad8af8 (2024).
81. Moradi, M., Heinz, A., Wagner, U. & Koch, T. Modeling the emissions of a gasoline engine during high-transient operation using machine learning approaches. *Int. J. Engine Res.* **23**(6), 1708–1716. https://doi.org/10.1177/14680874211032381 (2021).
82. Meresht, N. B., Munshi, S., Shahbakhti, M. & McTaggart-Cowan, G. Developing machine learning models to predict methane and nitrogen oxide engine-out emissions from a heavy-duty natural-gas engine. *Prog. Can. Mech. Eng.* https://doi.org/10.17118/11143/21169 (2023).
83. Brusa, A., Giovannardi, E., Barichello, M. & Cavina, N. Comparative evaluation of data-driven approaches to develop an engine surrogate model for NOx engine-out emissions under steady-state and transient conditions. *Energies* **15**(21), 8088. https://doi.org/10.3390/en15218088 (2022).
84. Pitchaiah, S., Juchelková, D., Sathyamurthy, R. & Atabani, A. E. Prediction and performance optimisation of a DI CI engine fuelled with diesel–bael biodiesel blends with DMC additive using RSM and ANN: Energy and exergy analysis. *Energy Convers. Manag.* **292**(July), 117386. https://doi.org/10.1016/j.enconman.2023.117386 (2023).

Author contributions
All authors have equally contributed to the manuscript.

Declarations

Competing interests
The authors declare no competing interests.

Additional information
Correspondence and requests for materials should be addressed to N.K.

Reprints and permissions information is available at www.nature.com/reprints.

Publisher's note Springer Nature remains neutral with regard to jurisdictional claims in published maps and institutional affiliations.